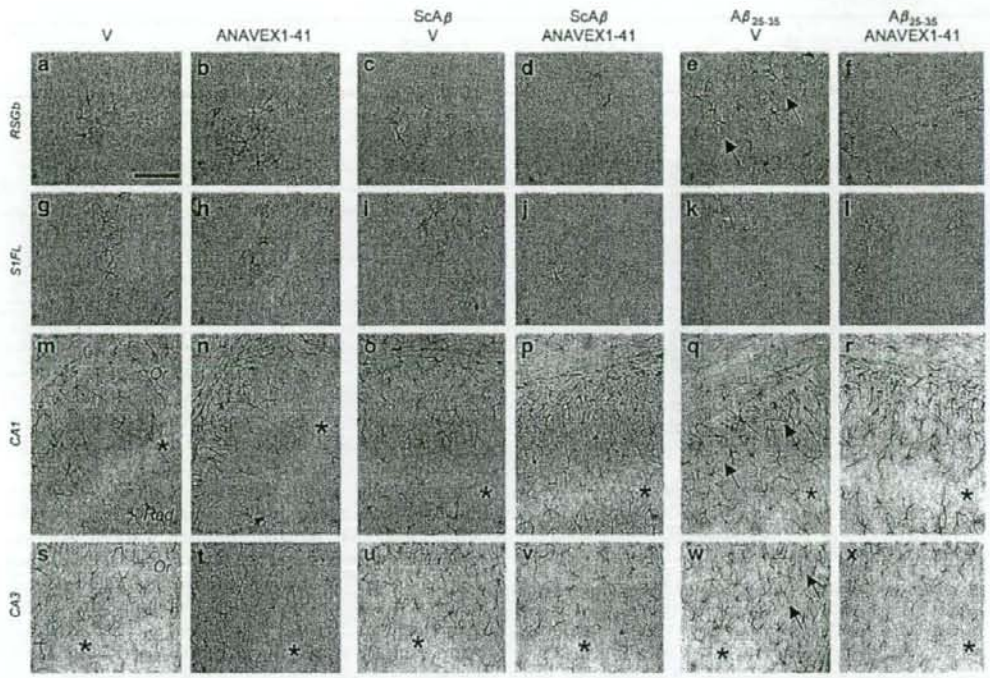

Figure 5 Morphological analysis of astrocytic reaction using GFAP immunolabeling in $A\beta_{25-35}$-treated mice. Animals were treated i.p. with saline vehicle solution (V) or ANAVEX1-41 (100 μg/kg) and received no i.c.v. treatment (two left columns), ScAβ (9 nmol; two central columns) or $A\beta_{25-35}$ (9 nmol; two right columns) and were killed after 7 days for immunohistological analysis. Coronal 30 μm thick sections were stained with anti-GFAP antibody and several brain areas were visually analyzed. Representative microphotographs are shown in two cortical areas, the retrospenial granular basal cortex (RSGb; a–f) and S1 cortex forelimb region (S1FL; g–l), and two hippocampal formation areas, the CA1 (m–r) and CA3 (s–x). The pyramidal cell layers are indicated by asterisks. Arrows outlined densifications of astrocyte labeling. Abbreviations: Or, oriens layer; Rad, stratum radiatum. At least three slices per mice and four mice per conditions were analyzed. Scale bar in (a) = 300 μm.

ANAVEX1-41, both in terms of step-down latency ($H = 39.7$, $p < 0.0001$; Figure 9c) and percentage of animals-to-criterion. The compound only nonsignificantly attenuated the ANAVEX1-41 (100 μg/kg) effect, particularly in terms of percentage of animals-to-criterion (Figure 9d), suggesting that protection through activation of σ_1 protein is differentially effective on short-term and long-term memory mechanisms.

DISCUSSION

The first data in this study showed that ANAVEX1-41 attenuated the learning deficits observed 1 week after the central injection of $A\beta_{25-35}$ peptide in mice. In the brain of rats or mice, $A\beta_{25-35}$ peptide induces, after acute injection or chronic infusion, biochemical changes, morphological alterations, and behavioral impairments reminiscent of AD physiopathology. In particular, $A\beta_{25-35}$-treated rodents showed spontaneous alternation, passive avoidance, and water-maze learning deficits (Maurice *et al*, 1996; Delobette *et al*, 1997) clearly related to alterations in cholinergic and glutamatergic corticolimbic systems (Maurice *et al*, 1996; Olariu *et al*, 2001). ANAVEX1-41, administered before the behavioral procedures, reversed the $A\beta_{25-35}$-induced deficits with a very low active dose range because the maximum antiamnesic effect was measured at 10 μg/kg for both the short-term and long-term memory tests. This observation confirms that ANAVEX1-41 is a very potent antiamnesic drug. The compound acts as a σ_1 protein activator, with a K_i value of 44 nM (Espallergues *et al*, 2007). Such pharmacological action is known to mediate antiamnesic effects, particularly against $A\beta_{25-35}$-induced learning impairments. Numerous σ_1 protein activators including (+)-SKF-10 047, (+)-pentazocine, SA4503, or PRE-084 attenuated $A\beta_{25-35}$-induced learning impairments (Maurice *et al*, 1998; Meunier *et al*, 2006). Indeed, activation of the σ_1 protein rapidly results in amplification of Ca^{2+} mobilization from intracellular stores, facilitating Ca^{2+}-dependent intracellular pathways and activation of intracellular kinases (Morin-Surun *et al*, 1999; Hayashi and Su, 2001; Dong *et al*, 2005). In turn, σ_1 protein activators increase hippocampus glutamatergic transmission by facilitating glutamate release, activation of glutamate receptors and long-term potentiation (Monnet *et al*, 1992; Dong *et al*, 2005). They may also directly facilitate cholinergic neurotransmission by inducing acetylcholine release in the

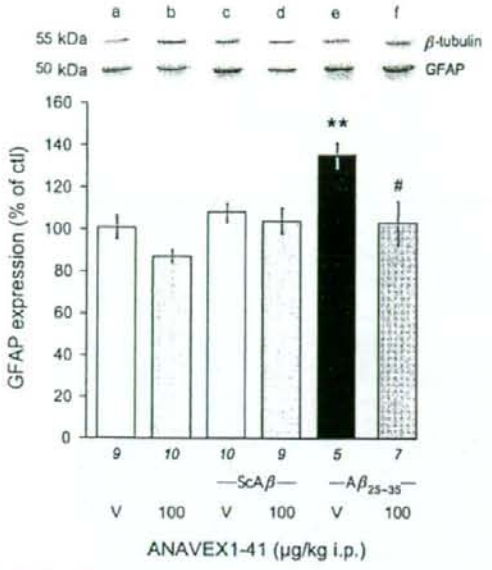

Figure 6 Effect of ANAVEX1-41 on GFAP expression measured by western blot in the hippocampus of $A\beta_{25-35}$-treated mice. Animals were treated i.p. with saline vehicle solution (V) or ANAVEX1-41 (100 μg/kg) and received no i.c.v. treatment (two left columns), $ScA\beta$ (9 nmol; two central columns) or $A\beta_{25-35}$ (9 nmol; two right columns) and were killed after 7 days for western blot analysis. GFAP 50 kDa variations were compared with untreated mice and normalized with β-tubulin expression levels. Typical micrographs are shown in the upper panel. The number of animals per group is indicated below each column. The number of animals per group is indicated below the columns. Lanes on the blots: *a*, V; *b*, ANAVEX1-41; *c*, $ScA\beta$ + V; *d*, $ScA\beta$ + ANAVEX1-41; *e*, $A\beta_{25-35}$ + V; *f*, $A\beta_{25-35}$ + ANAVEX1-41. **$p < 0.01$ *vs* the V-treated group; #$p < 0.05$ *vs* the ($A\beta_{25-35}$ + V)-treated group; Dunnett's test.

hippocampus and cortex (Matsuno *et al*, 1995; Horan *et al*, 2002).

ANAVEX1-41, however, also acts as a muscarinic ligand. We have previously reported that the compound shows K_i values in the low nanomolar range for muscarinic receptors subtypes (18–114 nM), with a profile by ascending order of potency: $M_1 > M_3 > M_4 > M_2$ (Espallergues *et al*, 2007). All subtypes of muscarinic receptors are expressed in the hippocampus and cortex (Levey *et al*, 1995) and post-synaptic M_1 and autoreceptor M_2 subtypes have been shown to be crucially involved in learning and memory processes (Ghelardini *et al*, 1999; but see also Quirion *et al*, 1995; Miyakawa *et al*, 2001; Seeger *et al*, 2004). Nonselective muscarinic antagonists, such as scopolamine and atropine, impair performance in various learning and memory tasks in rodents, including eight-arm radial maze learning (Eckerman *et al*, 1980), contextual fear conditioning (Anagnostaras *et al*, 1995), water-maze learning (Sutherland *et al*, 1982), or passive avoidance (Espallergues *et al*, 2007).

The combined activity of ANAVEX1-41 at σ_1 protein and muscarinic receptors is expected to lead to synergistic effect on memory. Indeed, activation of the σ_1 protein and M_2 autoreceptors antagonism by ANAVEX1-41 (Vamvakides, 2002; Espallergues *et al*, 2007) may facilitate Ca^{2+}-dependent acetylcholine release from presynaptic terminals in the hippocampus and cortex, as shown with other compounds (Quirion *et al*, 1995; Matsuno *et al*, 1995; Horan *et al*, 2002). As previously discussed (Espallergues *et al*, 2007), it is obvious that, at the very low pharmacologically active doses (10–100 μg/kg) measured for ANAVEX1-41, the compound acts both as σ_1 activator and muscarinic receptor ligand and provokes complex concomitant effects on neurotransmission that will affect: (i) acetylcholine release, by presynaptic σ_1 protein-mediated and M_2 autoreceptor-mediated effects; (ii) phospholipase C activation induced by muscarinic receptor activation but amplified by σ_1 protein-mediated activity; and (iii) IP_3 formation and activation of ER IP_3 receptors, again amplified by the σ_1 protein activation. Noteworthy, the active dose shown by ANAVEX1-41 is unrelated to the drug *in vitro* affinities for either σ_1 protein or muscarinic receptor subtypes. For comparison, PRE-084, a selective σ_1 activator with a similar affinity of 44 nM (Su *et al*, 1991), is antiamnesic at 0.5–1 mg/kg against $A\beta_{25-35}$-induced learning impairments (Meunier *et al*, 2006). One of the most promising muscarinic compound, AF102B, inhibiting ^{3}H-quinuclidinyl benzilate binding with K_i values in the 1–5 nM concentration range (Fisher *et al*, 1991), is active at 1–5 mg/kg against the learning deficits induced in rats by bilateral i.c.v. injection of the cholinotoxin ethylcholine aziridinium ion (AF64A; Nakahara *et al*, 1989). ANAVEX1-41, with a similar affinity for σ_1 protein as PRE-084 and even lower affinities for muscarinic subtypes as AF102B, showed an *in vivo* activity at 10 μg/kg, ie, almost 100 times lower than the cited drugs. These data must be tempered after considering the protein binding and brain/plasma ratio in humans, but suggests strong synergic effects between the σ_1 and muscarinic targets. The precise mechanism of action remains to be analyzed more adequately using *in vitro* preparations, but it clearly relies on facilitated Ca^{2+} mobilization and activation of Ca^{2+}-dependent intracellular signaling induced by muscarinic receptor and σ_1 protein during learning-induced neuronal activation.

The second part of the study analyzed the neuroprotective potential of ANAVEX1-41 in $A\beta_{25-35}$-treated mice. For this purpose, the compound was administered at the same time as $A\beta_{25-35}$, ie, 7 days before the behavioral, morphological or biochemical analyses, a procedure known to allow the observation of neuroprotective effects for mixed cholinergic and σ_1 drugs (Meunier *et al*, 2006). The compound induced a bell shaped but significant prevention of $A\beta_{25-35}$-induced learning deficits, with an active dose about 100 μg/kg. At the morphological level, $A\beta_{25-35}$ induced a limited but significant cell loss in the CA1 pyramidal cell layer of the hippocampus (Stepanichev *et al*, 2004) and a marked inflammation in corticolimbic structures that could be visualized by analyzing the GFAP immunolabeling in reactive astrocytes (Stepanichev *et al*, 2003; Klementiev *et al*, 2007). Interestingly, although a significant cell loss could be measured in particularly vulnerable areas, like CA1 in mice, GFAP immunolabeling increased in a more diffuse manner, in structures associated with the amyloid deposits, as observed in the retrospenial granular basal cortex and oriens layer of the hippocampus. ANAVEX1-41, tested at 100 μg/kg, significantly attenuated the $A\beta_{25-35}$-induced cell loss in CA1 and increase in GFAP expression, as shown by

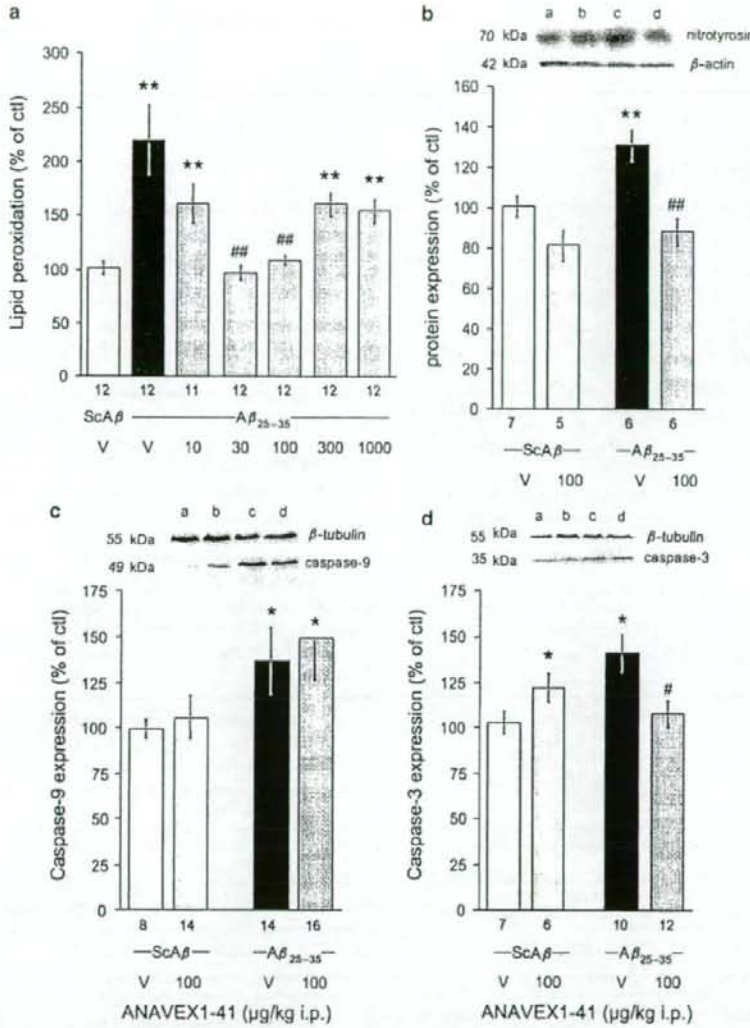

Figure 7 Neuroprotective effects of ANAVEX1-41 measured using biochemical markers in the hippocampus in $A\beta_{25-35}$ peptide-injected mice: (a) lipid peroxidation levels, (b) protein nitration levels; (c) caspase-9 expression; (d) caspase-3 expression. Mice were administered i.p. with saline vehicle solution (V) or ANAVEX1-41, 10–1000 µg/kg in (a) or 100 µg/kg in (b) and (c), 20 min before the i.c.v. injection of ScAβ or $A\beta_{25-35}$ peptide (9 nmol). Lipid peroxidation levels and caspases induction were measured on day 7 and protein nitration on day 5. The number of animals per group is indicated below the columns. Lanes on the blots: *a*, ScAβ + V; *b*, ScAβ + ANAVEX1-41; *c*, $A\beta_{25-35}$ + V; *d*, $A\beta_{25-35}$ + ANAVEX1-41. $^{*}p<0.05$, $^{**}p<0.01$ *vs* the (ScAβ + V)-treated group; $^{\#}p<0.05$, $^{\#\#}p<0.01$ *vs* the ($A\beta_{25-35}$ + V)-treated group; Dunnett's test.

western blot. It appeared then that ANAVEX1-41 is able to counteract the morphological damages induced by amyloid toxicity in sensitive structures.

The neuroprotective effect of the compound was also tested using selected biochemical markers. First, Aβ induces a strong oxidative stress, as observed in cell culture models (Behl *et al*, 1994) or in the hippocampus and cortex of rodents centrally injected with the peptides (Meunier *et al*, 2006). We therefore analyzed the level of lipid peroxidation in the hippocampus, 7 days after $A\beta_{25-35}$. Peroxynitrite anion, $ONOO^-$, is formed from nitric oxide and superoxide anion during oxidative stress and is responsible for a widespread biological damage in the AD brains (Smith *et al*, 1997). $A\beta_{25-35}$-induced formation of $ONOO^-$ could be indirectly indicated by the level of nitrated proteins, 5 days after peptide injection (Alkam *et al*, 2007). Moreover, Aβ-induced oxidative stress is because of production of reactive oxygen species by the mitochondria, by premature electron leakage to oxygen through the respiratory electron transport chain, and dysfunction of enzymes responsible for

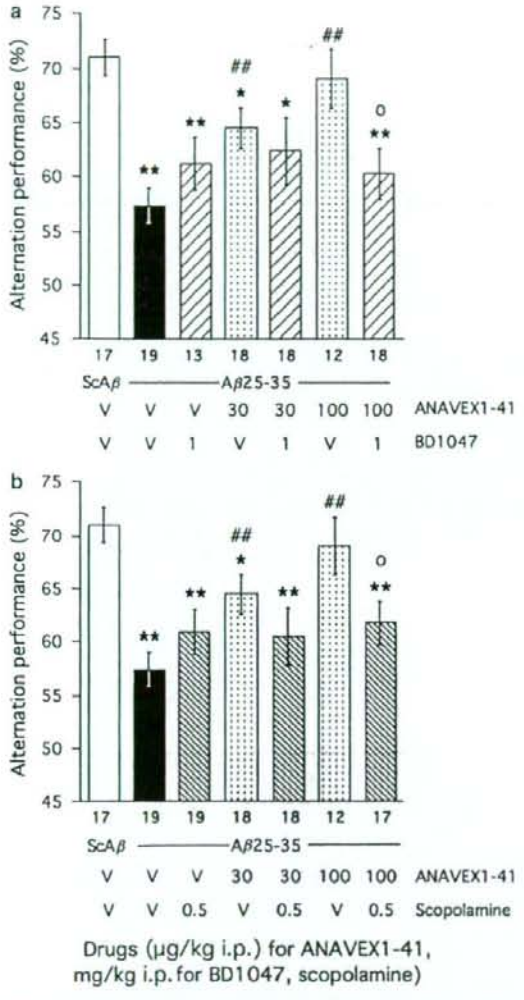

Figure 8 Effect of the preadministration of the muscarinic antagonist scopolamine (b) or the σ_1 receptor antagonist BD1047 (a) on the ANAVEX1-41 protective effect against the $A\beta_{25-35}$-induced alternation deficits in mice. Mice were administered i.p. with saline vehicle solution (V), scopolamine (0.5 mg/kg), BD1047 (1 mg/kg) and/or ANAVEX1-41 (30, 100 µg/kg), 20 min before ScAβ or $A\beta_{25-35}$ (9 nmol). After 7 days, they were examined for spontaneous alternation in the Y-maze. The number of animals per group is indicated below the columns. $^{*}p<0.05$, $^{**}p<0.01$ *vs* (ScAβ + V)-treated group; $^{\#\#}p<0.01$ *vs* ($A\beta_{25-35}$ + V)-treated group; $^{o}p<0.05$ *vs* ($A\beta_{25-35}$ + ANAVEX1-41)-treated group; Dunnett's test.

limiting the superoxide production, such as NAPDH-dependent oxidase, NADH-dependent diaphorase, and superoxide dismutase (Kim *et al*, 2003). Several markers could be used to selectively assess the appearance of mitochondrial damage, such as release of cytochrome *c* into the cytosol or, as we analyzed, induction of caspase-9. Finally, we also analyzed the induction of caspase-3, known to be a key mediator of Aβ-mediated apoptosis. Results showed that ANAVEX1-41 blocked the $A\beta_{25-35}$-induced increase in lipid peroxidation, at 30 and 100 µg/kg, in the hippocampus. The compound also blocked the increase in protein nitration. This antioxidant effect, however, may not primarily involve the mitochondria because $A\beta_{25-35}$-induced increase in caspase-9 was not attenuated by ANAVEX1-41. Noteworthy, the σ_1 protein is expressed at the surface of the mitochondria and at focal contacts between the ER and mitochondria (Hayashi and Su, 2007). We have previously observed that the σ_1 protein activator PRE-084 blocks the $A\beta_{25-35}$-induced increase in lipid peroxidation (Meunier *et al*, 2006), suggesting that activation of the σ_1 protein results in an antioxidant effect mediated at the mitochondrial level. Our biochemical data suggest that ANAVEX1-41 also induces a strong antioxidant effect that may, however, not primarily involve a protection of mitochondrial integrity through σ_1 protein activation. Otherwise, oxidative stress has been shown to impair M_1 and M_2 muscarinic receptor signaling activity, through increased phosphorylation and sequestration (Mou *et al*, 2006), an effect that may impede the pharmacological action of ANAVEX1-41 at muscarinic receptors. A precise mechanistic study has therefore to be carried out to identify the mechanism of the antioxidant action of ANAVEX1-41. The compound is nevertheless protective against the resulting apoptosis, as it blocked the induction of caspase-3. This observation could be considered as one of the cellular correlates of the protecting effect of ANAVEX1-41, already described at the morphological and behavioral levels.

The mechanism of the neuroprotective activity of ANAVEX1-41 is likely to involve, as detailed above regarding its antiamnesic action, a complex interaction between its muscarinic and σ_1 targets. We observed that scopolamine or BD1047 could significantly inhibit the protective effect of ANAVEX1-41, at least in terms of learning deficits. A synergistic σ_1/muscarinic mechanism could also be evoked to account for the neuroprotective efficacy of ANAVEX1-41, in particular, through the phospholipase C involvement and regulation of intracellular Ca^{2+} homeostasis.

In summary, we reported that ANAVEX1-41, a new mixed muscarinic receptor ligand and σ_1 protein activator, is a very active antiamnesic and neuroprotective drug against $A\beta_{25-35}$ peptide-induced amnesia and toxicity in the mouse. Its similar efficacy at muscarinic and σ_1 targets suggest a unique, concomitant action, most probably at the presynaptic and intraneuronal levels, on neurotransmitter release, activation of membrane receptors and intracellular transduction systems.

ACKNOWLEDGEMENTS

This work was supported by collaboration contracts (no. 06122, no. 07438) between Anavex Life Sciences and INSERM (Paris, France); by grants of the 'Academic Frontier' Project for private universities (2007–2011) from the Ministry of Education, Culture, Sports, Sciences, and Technology of Japan; and by an exchange program between the Japanese Society for the Promotion of Science (Tokyo, Japan) and INSERM.

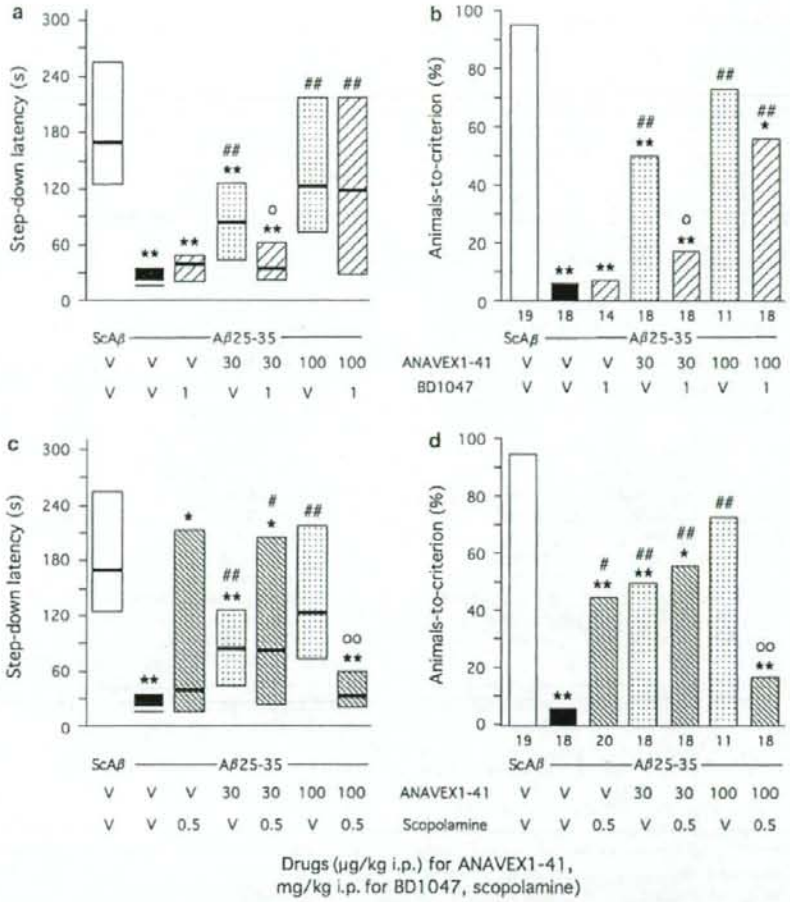

Figure 9 Effect of the preadministration of scopolamine (c, d) or BD1047 (a, b) on the ANAVEX1-41 effect against the $A\beta_{25-35}$-induced passive avoidance deficits in mice: step-down latency (a, c) and percentage of animals-to-criterion (b, d). Mice were administered i.p. with saline vehicle solution (V), scopolamine (0.5 mg/kg), BD1047 (1 mg/kg), and/or ANAVEX1-41 (30, 100 μg/kg), 20 min before ScAβ or $A\beta_{25-35}$ (9 nmol). They were trained on day 7 and retention was performed on day 8. The number of animals is indicated below the columns. $^{*}p<0.05$, $^{**}p<0.01$ *vs* (ScAβ + V)-treated group; $^{\#}p<0.05$, $^{\#\#}p<0.01$ *vs* ($A\beta_{25-35}$ + V)-treated group; $^{o}p<0.05$, $^{oo}p<0.01$ *vs* ($A\beta_{25-35}$ + ANAVEX1-41)-treated group; Dunn's test in (a) and (c), χ^2-test in (b) and (d).

DISCLOSURE/CONFLICT OF INTEREST

T Maurice is a member of the scientific advisory board of Anavex Life Sciences. Other authors declare that, except for income received from their primary employer, no financial support or compensation has been received from any individual or corporate entity for research or professional service and there are no personal financial holdings that could be perceived as constituting a potential conflict of interest.

REFERENCES

Abramov AY, Canevari L, Duchen MR (2004). β-Amyloid peptides induce mitochondrial dysfunction and oxidative stress in astrocytes and death of neurons through activation of NADPH oxidase. *J Neurosci* **24**: 565–575.

Alkam T, Nitta A, Mizoguchi H, Itoh A, Nabeshima T (2007). A natural scavenger of peroxynitrites, rosmarinic acid, protects against impairment of memory induced by $A\beta_{25-35}$. *Behav Brain Res* **180**: 139–145.

Anagnostaras SG, Maren S, Fanselow MS (1995). Scopolamine selectively disrupts the acquisition of contextual fear conditioning in rats. *Neurobiol Learn Mem* **64**: 191–194.

Behl C, Davis JB, Lesley R, Schubert D (1994). Hydrogen peroxide mediates amyloid β protein toxicity. *Cell* **77**: 817–827.

Chafekar SM, Baas F, Scheper W (2008). Oligomer-specific Aβ toxicity in cell models is mediated by selective uptake. *Biochim Biophys Acta* **1782**: 523–531.

Chafekar SM, Hoozemans JJ, Zwart R, Baas F, Scheper W (2007). $A\beta_{1-42}$ induces mild endoplasmic reticulum stress in an aggregation state-dependent manner. *Antioxid Redox Signal* **9**: 2245–2254.

Delobette S, Privat A, Maurice T (1997). *In vitro* aggregation facilities beta-amyloid peptide-(25–35)-induced amnesia in the rat. *Eur J Pharmacol* **319**: 1–4.

Dong Y, Fu YM, Sun JL, Zhu YH, Sun FY, Zheng P (2005). Neurosteroid enhances glutamate release in rat prelimbic cortex via activation of α_1-adrenergic and σ_1 receptors. *Cell Mol Life Sci* 62: 1003–1104.

Eckerman DA, Gordon WA, Edwards JD, MacPhail RC, Gage MI (1980). Effects of scopolamine, pentobarbital, and amphetamine on radial arm maze performance in the rat. *Pharmacol Biochem Behav* 12: 595–602.

Eikelenboom P, Bate C, Van Gool WA, Hoozemans JJ, Rozemuller JM, Veerhuis R *et al* (2002). Neuroinflammation in Alzheimer's disease and prion disease. *Glia* 40: 232–239.

Espallergues J, Lapalud P, Christopoulos A, Avlani VA, Sexton PM, Vamvakides A *et al* (2007). Involvement of the sigma$_1$ (σ_1) receptor in the anti-amnesic, but not antidepressant-like, effects of the aminotetrahydrofuran derivative ANAVEX1-41. *Br J Pharmacol* 152: 267–279.

Fang F, Liu GT (2006). Protective effects of compound FLZ on β-amyloid peptide-(25–35)-induced mouse hippocampal injury and learning and memory impairment. *Acta Pharmacol Sin* 27: 651–658.

Fisher A, Brandeis R, Karton I, Pittel Z, Gurwitz D, Haring R *et al* (1991). (+−)-*cis*-2-Methyl-spiro(1,3-oxathiolane-5,3′)quinuclidine, an M$_1$ selective cholinergic agonist, attenuates cognitive dysfunctions in an animal model of Alzheimer's disease. *J Pharmacol Exp Ther* 257: 392–403.

Frederickson RC (1992). Astroglia in Alzheimer's disease. *Neurobiol Aging* 13: 239–253.

Ghelardini C, Galeotti N, Matucci R, Bellucci C, Gualtieri F, Capaccioli S *et al* (1999). Antisense 'knockdowns' of M1 receptors induce transient anterograde amnesia in mice. *Neuropharmacology* 38: 339–348.

Gruden MA, Davidova TB, Malisauskas M, Sewell RD, Voskresenskaya NI, Wilhelm K *et al* (2007). Differential neuroimmune markers to the onset of Alzheimer's disease neurodegeneration and dementia: autoantibodies to Aβ_{25-35} oligomers, S100 β and neurotransmitters. *J Neuroimmunol* 186: 181–192.

Hayashi T, Su TP (2001). Regulating ankyrin dynamics: roles of sigma-1 receptors. *Proc Natl Acad Sci USA* 98: 491–496.

Hayashi T, Su TP (2003). Sigma-1 receptors (σ_1 binding sites) form raft-like microdomains and target lipid droplets on the endoplasmic reticulum: roles in endoplasmic reticulum lipid compartmentalization and export. *J Pharmacol Exp Ther* 306: 718–725.

Hayashi T, Su TP (2007). Sigma-1 receptor chaperones at the ER-mitochondrion interface regulate Ca^{2+} signaling and cell survival. *Cell* 131: 596–610.

Horan B, Gifford AN, Matsuno K, Mita S, Ashby Jr CR (2002). Effect of SA4503 on the electrically evoked release of ^{3}H-acetylcholine from striatal and hippocampal rat brain slices. *Synapse* 46: 1–3.

Kim HC, Yamada K, Nitta A, Olariu A, Tran MH, Mizuno M *et al* (2003). Immunocytochemical evidence that amyloid β_{1-42} impairs endogenous antioxidant systems *in vivo*. *Neuroscience* 119: 399–419.

Klementiev B, Novikova T, Novitskaya V, Walmod PS, Dmytriyeva O, Pakkenberg B *et al* (2007). A neural cell adhesion molecule-derived peptide reduces neuropathological signs and cognitive impairment induced by Aβ_{25-35}. *Neuroscience* 145: 209–224.

Kubo T, Nishimura S, Kumagae Y, Kaneko I (2002). *In vivo* conversion of racemized β-amyloid ([D-Ser^{26}]Aβ_{1-40}) to truncated and toxic fragments ([D-Ser^{26}]A$\beta_{25-35/40}$) and fragment presence in the brains of Alzheimer's patients. *J Neurosci Res* 70: 474–483.

Kuboyama T, Tohda C, Komatsu K (2006). Withanoside IV and its active metabolite, sominone, attenuate Aβ_{25-35}-induced neurodegeneration. *Eur J Neurosci* 23: 1417–1426.

Levey AI, Edmunds SM, Koliatsos V, Wiley RG, Heilman CJ (1995). Expression of m1–m4 muscarinic acetylcholine receptor proteins in rat hippocampus and regulation by cholinergic innervation. *J Neurosci* 15: 4077–4092.

Marrazzo A, Caraci F, Salinaro ET, Su TP, Copani A, Ronsisvalle G (2005). Neuroprotective effects of sigma-1 receptor agonists against β-amyloid-induced toxicity. *Neuroreport* 16: 1223–1226.

Matsuno K, Senda T, Kobayashi T, Mita S (1995). Involvement of sigma$_1$ receptor in (+)-*N*-allylnormetazocine-stimulated hippocampal cholinergic functions in rats. *Brain Res* 60: 200–206.

Mattson MP, Cheng B, Davis D, Bryant K, Lieberburg I, Rydel RE (1992). β-Amyloid peptides destabilize calcium homeostasis and render human cortical neurons vulnerable to excitotoxicity. *J Neurosci* 12: 376–389.

Maurice T, Grégoire C, Espallergues J (2006). Neuro(active)steroids actions at the neuromodulatory sigma$_1$ (σ_1) receptor: biochemical and physiological evidences, consequences in neuroprotection. *Pharmacol Biochem Behav* 84: 581–597.

Maurice T, Lockhart BP, Privat A (1996). Amnesia induced in mice by centrally administered beta-amyloid peptides involves cholinergic dysfunction. *Brain Res* 706: 181–193.

Maurice T, Su TP, Privat A (1998). Sigma$_1$ (σ_1) receptor agonists and neurosteroids attenuate β_{25-35}-amyloid peptide-induced amnesia in mice through a common mechanism. *Neuroscience* 83: 413–428.

Meunier J, Ieni J, Maurice T (2006). The anti-amnesic and neuroprotective effects of donepezil against amyloid β_{25-35} peptide-induced toxicity in mice involve an interaction with the σ_1 receptor. *Br J Pharmacol* 149: 998–1012.

Miyakawa T, Yamada M, Duttaroy A, Wess J (2001). Hyperactivity and intact hippocampus-dependent learning in mice lacking the M1 muscarinic acetylcholine receptor. *J Neurosci* 21: 5239–5250.

Monnet FP, Debonnel G, de Montigny C (1992). *In vivo* electrophysiological evidence for a selective modulation of *N*-methyl-D-aspartate-induced neuronal activation in rat CA3 dorsal hippocampus by sigma ligands. *J Pharmacol Exp Ther* 261: 123–130.

Monnet FP, Maurice T (2006). The sigma$_1$ protein as a target for the non-genomic effects of neuro(active)steroids: molecular, physiological, and behavioral aspects. *J Pharmacol Sci* 100: 93–118.

Morin-Surun MP, Collin T, Denavit-Saubié M, Baulieu EE, Monnet FP (1999). Intracellular sigma$_1$ receptor modulates phospholipase C and protein kinase C activities in the brainstem. *Proc Natl Acad Sci USA* 96: 8196–8199.

Mou L, Gates A, Mosser VA, Tobin A, Jackson DA (2006). Transient hypoxia induces sequestration of M$_1$ and M$_2$ muscarinic acetylcholine receptors. *J Neurochem* 96: 510–519.

Nakahara N, Iga Y, Saito Y, Mizobe F, Kawanishi G (1989). Beneficial effects of FKS-508 (AF102B), a selective M$_1$ agonist, on the impaired working memory in AF64A-treated rats. *Jpn J Pharmacol* 51: 539–547.

Olariu A, Tran MH, Yamada K, Mizuno M, Hefco V, Nabeshima T (2001). Memory deficits and increased emotionality induced by β-amyloid$_{25-35}$ are correlated with the reduced acetylcholine release and altered phorbol dibutyrate binding in the hippocampus. *J Neural Transm* 108: 1065–1079.

Quirion R, Wilson A, Rowe W, Aubert I, Richard J, Doods H *et al* (1995). Facilitation of acetylcholine release and cognitive performance by an M$_2$-muscarinic receptor antagonist in aged memory-impaired. *J Neurosci* 15: 1455–1462.

Seeger T, Fedorova I, Zheng F, Miyakawa T, Koustova E, Gomeza J *et al* (2004). M2 muscarinic acetylcholine receptor knock-out mice show deficits in behavioral flexibility, working memory, and hippocampal plasticity. *J Neurosci* 24: 10117–10127.

Selkoe DJ (1989). Molecular pathology of amyloidogenic proteins and the role of vascular amyloidosis in Alzheimer's disease. *Neurobiol Aging* 10: 387–395.

Selkoe DJ (2004). Cell biology of protein misfolding: the examples of Alzheimer's and Parkinson's diseases. *Nat Cell Biol* 6: 1054–1061.

Smith MA, Richey Harris PL, Sayre LM, Beckman JS, Perry G (1997). Widespread peroxynitrite-mediated damage in Alzheimer's disease. *J Neurosci* **17**: 2653–2657.

Stepanichev MY, Moiseeva YV, Lazareva NA, Onufriev MV, Gulyaeva NV (2003). Single intracerebroventricular administration of amyloid-β_{25-35} peptide induces impairment in short-term rather than long-term memory in rats. *Brain Res Bull* **61**: 197–205.

Stepanichev MY, Zdobnova IM, Zarubenko II, Lazareva NA, Gulyaeva NV (2006). Studies of the effects of central administration of β-amyloid peptide (25–35): pathomorphological changes in the hippocampus and impairment of spatial memory. *Neurosci Behav Physiol* **36**: 101–106.

Stepanichev MY, Zdobnova IM, Zarubenko II, Moiseeva YV, Lazareva NA, Onufriev MV *et al* (2004). Amyloid-β_{25-35}-induced memory impairments correlate with cell loss in rat hippocampus. *Physiol Behav* **80**: 647–655.

Su TP, Wu XZ, Cone EJ, Shukla K, Gund TM, Dodge AL *et al* (1991). Sigma compounds derived from phencyclidine: identification of PRE-084, a new, selective sigma ligand. *J Pharmacol Exp Ther* **259**: 543–550.

Sutherland RJ, Whishaw IQ, Regehr JC (1982). Cholinergic receptor blockade impairs spatial localization by use of distal cues in the rat. *J Comp Physiol Psychol* **96**: 563–573.

Um MY, Choi WH, Aan JY, Kim SR, Ha TY (2006). Protective effect of *Polygonum multiflorum* Thunb on amyloid β-peptide 25–35 induced cognitive deficits in mice. *J Ethnopharmacol* **104**: 144–148.

Vamvakides A (2002). Mechanism of action of tetrahydro-*N*,*N*-dimethyl-5,5-diphenyl-3-furanemethanamine, a putative nootropic, anti-epileptic and antidepressant compound. *Ann Pharm Fr* **60**: 415–422.

Walsh DM, Klyubin I, Fadeeva JW, Cullen WK, Anwyl R, Wolfe MS *et al* (2002). Naturally secreted oligomers of amyloid β protein potently inhibit hippocampal long-term potentiation *in vivo*. *Nature* **416**: 535–539.

Supplementary Information accompanies the paper on the Neuropsychopharmacology website (http://www.nature.com/npp)

Available online at www.sciencedirect.com
ScienceDirect
Behavioural Brain Research 189 (2008) 100–106
BEHAVIOURAL BRAIN RESEARCH
www.elsevier.com/locate/bbr

Research report

Restraining tumor necrosis factor-alpha by thalidomide prevents the Amyloid beta-induced impairment of recognition memory in mice

Tursun Alkam[a,d], Atsumi Nitta[a], Hiroyuki Mizoguchi[a,e], Kuniaki Saito[b], Mitsuru Seshima[c], Akio Itoh[a], Kiyofumi Yamada[a], Toshitaka Nabeshima[a,f,g,*]

[a] Department of Neuropsychopharmacology & Hospital Pharmacy, Nagoya University Graduate School of Medicine, Nagoya 466-8560, Japan
[b] Human Health Science, Graduate School of Medicine and Faculty of Medicine, Kyoto University, Kyoto 606-8507, Japan
[c] Department of Informative Clinical Medicine, Gifu University Graduate School of Medicine, Gifu 501-1194, Japan
[d] Department of Basic Medicine, College of Traditional Uighur Medicine, Hotan 848-000, China
[e] Futuristic Environmental Simulation Center, Research Institute of Environmental Medicine, Nagoya University, Nagoya 464-8601, Japan
[f] Japanese Drug Organization of Appropriate Use and Research, Nagoya 468-0069, Japan
[g] Department of Chemical Pharmacology, Graduate School of Pharmaceutical Science, Meijo University, Nagoya 468-8503, Japan

Received 13 December 2007; accepted 17 December 2007
Available online 27 December 2007

Abstract

No effective remedy has currently been realized to prevent the cognitive impairments of Alzheimer's disease (AD). The interruption of the toxic pathways of amyloid beta peptide (Aβ) still remains promising for the treatment. The involvement of tumor necrosis factor-alpha (TNF-α) in the toxicity of $A\beta_{1-40}$ in recent reports provide a fresh target for the interruption. In the current study, we evaluated the feasibility of a strategy that target TNF-α to prevent the impairment of memory induced by Aβ. The *i.c.v*-injection of $A\beta_{25-35}$ increased the hippocampal mRNA expression of both TNF-α and inducible nitric oxide synthase (iNOS), of which the former was stronger. The knock-out of TNF-α (TNF-α (−/−)) in mouse prevented the increase of iNOS mRNA induced by $A\beta_{25-35}$. Not only the inhibition of iNOS activity but also TNF-α (−/−) prevented the nitration of proteins in the hippocampus and the impairment of recognition memory in mice induced by $A\beta_{25-35}$. Daily treatment with thalidomide (20 mg/kg), a preferential degrader of TNF-α mRNA, or *i.c.v.*-injection of an anti-TNF-α antibody (10 ηg/mouse) prevented the nitration of proteins in the hippocampus and the impairment of recognition memory induced by $A\beta_{25-35}$ or $A\beta_{1-40}$ in mice. These results suggested the practicability of targeting TNF-α as a preventive strategy against Aβ-mediated cognitive impairments.

Keywords: Amyloid beta ($A\beta_{25-35}$); Tumor necrosis factor-alpha; Protein nitration; Recognition memory; Thalidomide

1. Introduction

Treating the cognitive impairments of Alzheimer's disease (AD) is a complex practice due to its multifactoral pathology that including the increase of toxic amyloid beta peptide (Aβ), neuroinflammation, oxidative damage, and neurodegeneration in critical brain regions involved in memory and cognition [18,42,49,53,63,66]. Although, there have been many recent advances in the understandings of the pathological process of AD, therapeutic approaches still remain limited to targeting the toxic pathways of Aβ, the assumed central player in the pathogenesis of the disease [15,19,30,38,39,41,50].

The neurotoxicity of Aβ has recently been implicated by the involvement of tumor necrosis factor-alpha (TNF-α), a multifunctional cytokine that triggers a wide range of cellular responses [35]. TNF-α is found upregulated in AD patients [8,17,43,56], and involved in $A\beta_{1-40}$-induced inhibition of long-term potentiation in hippocampal slices and the impairment of spatial memory in mice [36,65]. $A\beta_{1-40}$ induces toxicity by a mechanism of TNF-α dependent overexpression of inducible nitric oxide synthase (iNOS) [2,13,69]. In general, TNF-α is regarded as an inducer of the expression of iNOS [11,23,51]. The induced iNOS produces high amount of NO [25,59] which interacts rapidly with superoxide to form prox-

* Corresponding author at: Department of Chemical Pharmacology, Graduate School of Pharmaceutical Science, Meijo University, Nagoya 468-8503, Japan Tel.: +81 52 835 2735; fax: +81 52 839 2735.
E-mail address: tnabeshi@ccmfs.meijo-u.ac.jp (T. Nabeshima).

0166-4328/$ – see front matter © 2007 Elsevier B.V. All rights reserved.
doi:10.1016/j.bbr.2007.12.014

ynitrite [6,46]. Proxynitrite mediates the extensive nitration of proteins in the brain of AD and evidently correlated with the increased level of cerebral Aβ and the severity of cognitive impairment [27,28,54,57]. The impairments of memory induced by Aβ in mice are prevented by the genetic deletion of TNF-α receptor or iNOS as well as by scavenging of peroxynitrite [3,36,40]. The implications of the involvement of TNF-α in iNOS-driven peroxynitrite and memory failure prompt a fresh strategy of targeting the synthesis of TNF-α for the prevention of Aβ-induced cognitive impairment. In this study, we have reconfirmed the critical involvement of TNF-α in the neurotoxicity of $A\beta_{25-35}$, the most toxic Aβ fragment that detected in the brain of AD patient [29,44,68], by utilizing TNF-α (−/−) mouse and evaluated the usefulness of targeting TNF-α by using thalidomide to prevent the Aβ-induced impairment of memory in mice.

2. Material and methods

2.1. Animals

Male C57BL/6 (wild type, WT) mice, male TNF-α knock out (TNF-α (−/−)) mice [55], and male ICR mice (Nihon SLC Co., Shizuoka, Japan), were used. The animals were housed in a controlled environment (23 ± 1 °C, 50 ± 5% humidity) and allowed food and water ad lib. The room lights were kept on between 8:00 .a.m and 8:00 p.m. All experiments were performed in accordance with the guidelines for animal experiments of Nagoya University Graduate School of Medicine. The procedures involving animals and their care conformed to the international guidelines set out in "Principles of Laboratory Animal Care".

2.2. Treatment and experimental design

$A\beta_{25-35}$ and $A\beta_{35-25}$ (Bachem, Bubendorf, Switzerland) were dissolved in sterile double-distilled water in a concentration of 1 mg/ml and stored at −20 °C before use and incubated for aggregation at 37 °C for 4 days before the injection. $A\beta_{1-40}$ and $A\beta_{40-1}$ (Bachem, Bubendorf, Switzerland) were dissolved in 35% acetonitrile/0.1% trifluoroacetic acid to a stock concentration of 1 mg/ml and stored at −20 °C before use. Peptides including $A\beta_{25-35}$ and $A\beta_{35-25}$ were *i.c.v.*- injected at a volume of 3 μl. Peptides including $A\beta_{40-1}$ and $A\beta_{1-40}$ were *i.c.v.*-injected at a volume of 5 μl. $A\beta_{35-25}$ and $A\beta_{40-1}$ were injected as the control. All peptides were injected as described previously [3,34]. Aminoguanidine (Wako, Saitama, Japan) was dissolved in saline and *i.p.*-injected at the dose of 100 mg/kg/day as described previously [36,59]. Thalidomide (Sigma, St. Louis, MO) was dissolved in dimethyl sulfoxide (DMSO) and *p.o.*-administrated at the dose of 20 mg/kg/day that was selected according to the previous literature on its pharmacodynamic study in mice [12]. Anti-TNF-α antibody (α-TNF-α) (R&D Systems, Minneapolis, MN) was *i.c.v.*-injected at the dose of 10 ηg that followed by the injection of Aβ peptides with 15 min interval as described previously [36]. The schedule of administration of peptides and drugs as well as biochemical and behavioral investigations are shown in Fig. 1.

2.3. Real-time reverse transcription-polymerase chain reaction

Mice were decapitated at the indicated time-points after the *i.c.v.*-injection of $A\beta_{25-35}$ (day 0). The hippocampi were removed on ice-cold glass plate and stored at −80 °C. The hippocampal tissue was homogenized and total RNA was extracted using an RNeasy total RNA isolation kit, following the supplier's protocol (Qiagen, Valencia, CA). cDNA was synthesized by using a Superscript™ reverse transcriptase kit (Invitrogen, Carlsbad, CA). The primer sequences were given below: for iNOS (Gene Bank access: NM_010927), forward primer: 5′-GGGCAGCCTGTGAGACCTT-3′; reverse primer: 5′-GCATTGGAAGTGAAGCGTTTC-3′; TaqMan probe: TGTCCGAAGCAAACATCACATTCAGATCC; For TNF-α (Gene Bank access: NM_023517), forward primer: 5′-CTTTCGGTTGCTCTTTGGTTGAG-3′; reverse primer: 5′-GCAGCTCTGTCTGTTGGATCAG-3′; TaqMan probe: TGCGACAGCAAAGTCACAGCCCC; for the brain-derived neurotrophic factor (BDNF) (Gene Bank access: BC034862), forward primer: 5′-GCAAACATGTCTATGAGGGTTCG-3′; reverse primer: 5′-ACTCGCTAATACTGTCACACACG-3′; TaqMan probe: ACTCCGACCCTGCCCGCCGT; for glial cell-derived neurotrophic factor (GDNF) (Gene Bank access: NM_010275), forward primer: 5′- GAAGAGAGAGGAATCGGCAGG-3′; reverse primer: 5′-TGGCCTCTGCGACCTTTC-3′; TaqMan probe: AGCTGCCAGCCCAGAGAATTCCAGAG; For all, the experimental amplification protocol consisted of a first round at 95 °C for 3 min and then 30 cycles of denaturation at 95 °C for 60 s, annealing at 60 °C for 60 s, and extension at 72 °C for 1 min, with a final extension reaction carried out at 72 °C for 10 min. PCR was carried out on Bio-Rad iCycler iQ™ real-time PCR detection system (Bio-Rad Laboratories, Hercules, CA). The signal was detected according to the manufacturer's instructions. The expression levels were calculated as described previously [62].

2.4. Western blotting

Animals were decapitated on day 7 after the injection of Aβ peptides. The hippocampi were removed on ice-cold glass plate and stored at −80 °C. The hippocampal tissues were homogenized as described previously [3]. Briefly, the hippocampal tissues were homogenized in ice-cold extraction buffer (150 μl of 20 mM Tris–HCl buffer (pH 7.6) containing 150 mM NaCl, 2 mM EDTA · 2Na, 50 mM sodium fluoride, 1 mM sodium vanadate, 1% NP-40, 1% sodium deoxycholate, 0.1% sodium dodecyl sulphate (SDS), 1 mg/ml pepstatin, 1 mg/ml aprotinin, and 1 mg/ml leupeptin). Equal amounts of protein, 20 μg/lane, were resolved by a 10% SDS-polyacrylamide gel electrophoresis, and then transferred electrophoretically to a polyvinylidene difluoride membrane (Millipore Corporation, Billerica, MA). Membranes were incubated in 3% skim milk in a washing buffer (Tris-buffered saline containing 0.05% (v/v) Tween-20) for 2 h at room temperature. Then the membranes were incubated at 4 °C overnight with a diluted (1:1000) anti-nitrotyrosine mouse clone1A6 (Upstate cell signaling, Lake Placid, USA) or with goat anti-actin primary antibody (1:100) (Santa Cruz Biotechnology Inc., Santa Crutz, CA). After a wash, membranes were incubated with horseradish peroxidase-labeled anti-mouse IgG (1:2000) (Kirkegaard & Perry Laboratories, Baltimore, MD) or with donkey anti-goat IgG secondary antibody (1:2000) (Santa Cruz Biotechnology Inc., Santa Crutz, CA). Immunoreactive complexes on the membrane were detected using Western blotting detection reagents (Amersham Biosciences Inc., Piscataway, NJ) according to the manufacturer's instructions, and exposed to X-ray film. The intensity of each protein band on the film, analyzed with the Atto Densitograph 4.1 system (Atto, Tokyo, Japan), and was corrected with the corresponding β-actin level. The results were expressed as the percentage of that of the control.

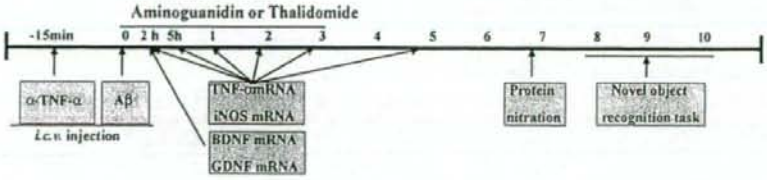

Fig. 1. The experimental schedule.

2.5. Novel object recognition task

This task, based on the spontaneous tendency of rodents to explore a novel object more often than a familiar one [16], was performed during Day 8–Day 10 after the *i.c.v.* injection of Aβ peptides as described previously [3]. A plastic chamber (35 × 35 × 35 cm) was used in low light condition during the light phase of the light/dark cycle. The general procedure consisted of three different phases: a habituation phase, an acquisition phase, and a retention phase. On the first day (habituation phase), mice were individually subjected to a single familiarization session of 10 min, during which they were introduced in the empty arena, in order to become familiar with the apparatus. On the second day (acquisition phase) animals were subjected to a single 10 min session, during which floor-fixed two objects (A and B) were placed in a symmetric position from the centre of the arena, 15 cm from each and 8 cm from the nearest wall. The two objects, made of the same wooden material with the similar color and smell, were different in shape but identical in size. Mice were allowed to explore the objects in the open field. A preference index for each mouse was expressed as a ratio of the amount of time spent exploring object A (TA × 100)/(TA + TB), where TA and TB are the time spent on exploring object A and object B, respectively. On the third day (retention phase), mice were allowed to explore the open field in the presence of two objects: the familiar object A and a novel object C in different shape but in similar color and size (A and C). A recognition index, calculated for each mouse, was expressed as the ratio (TC × 100)/(TA + TC), where TA and TC are the time spent during retention phase on object A and object C, respectively. The time spent exploring the object (nose pointing toward the object at a distance ≤1 cm) was recorded by hand.

2.6. Statistical analyses

The results are expressed as the mean ± S.E. Statistical significance was determined with one-way ANOVA followed by the Bonferroni multiple comparisons test. $p < 0.05$ was taken as a significant level of difference.

3. Results

3.1. TNF-α was involved in $A\beta_{25-35}$-induced impairment of recognition memory

The expression of TNF-α and iNOS mRNA in the hippocampus of mice was investigated at different time points after the *i.c.v.*-injection of $A\beta_{25-35}$. At 2 h time point, $A\beta_{25-35}$ increased the mRNA expressions of TNF-α and iNOS, the expression of the former was stronger than that of the latter (Fig. 2A). $A\beta_{25-35}$ did not increase the expression of iNOS mRNA in TNF-α (−/−) mouse at the two-hour time point (Fig. 2B).

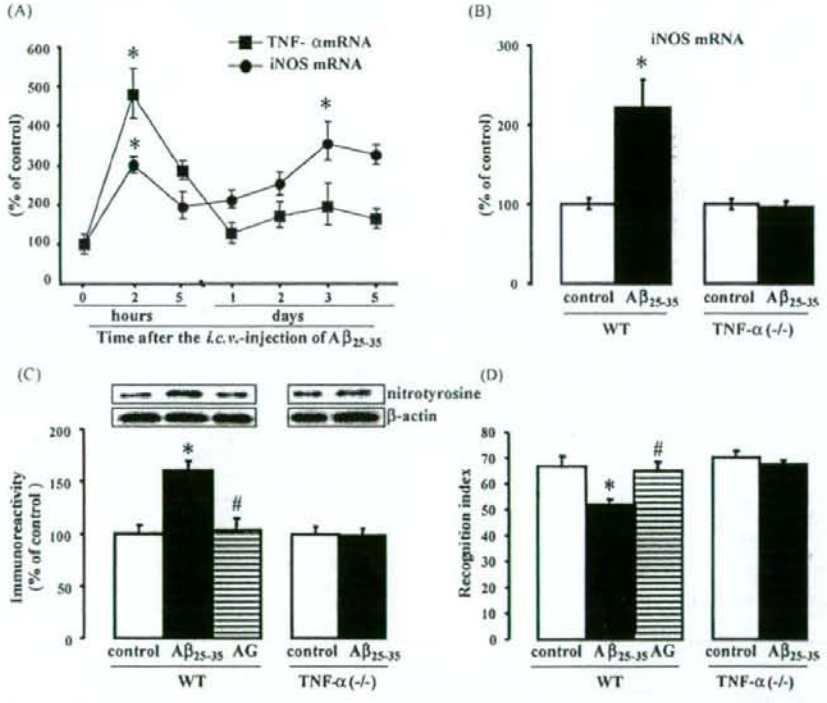

Fig. 2. TNF-α is required for the iNOS-mediated nitration of proteins and impairment of memory induced by $A\beta_{25-35}$. At different time points after the *i.c.v.*-injection of $A\beta_{25-35}$ (day 0) in mice, the mRNA expression levels of TNF-α and iNOS in the hippocampus were investigated by using real-time RT-PCR. A: $A\beta_{25-35}$ induced a sharp increase of TNF-α and iNOS mRNA in two hours after injection, the expression of the former was stronger than that of the latter. Data were presented as the mean ± S.E. ($n = 4$). * $p < 0.05$ vs. control. B: TNF-α (−/−) prevented the increase of iNOS mRNA which was induced by $A\beta_{25-35}$ in WT mice. Data were presented as the mean ± S.E. ($n = 4$). * $p < 0.05$ vs. control. C–D: Either the selective inhibition of iNOS activity by AG or TNF-α (−/−) prevented the $A\beta_{25-35}$-induced nitration of proteins in the hippocampus (day 7) and the impairment of novel object recognition memory (day 8–10). Data were presented as the mean ± S.E., ($n = 4$ for C, $n = 10$ for D), * $p < 0.05$ vs. control, # $p < 0.05$ vs. $A\beta_{25-35}$; TNF-α: tumor necrosis factor-alpha; iNOS: inducible nitric oxide synthase; WT: wild type; TNF-α (−/−): TNF-α knock out; AG: aminoguanidine; $A\beta_{25-35}$: Amyloid beta peptide (25–35).

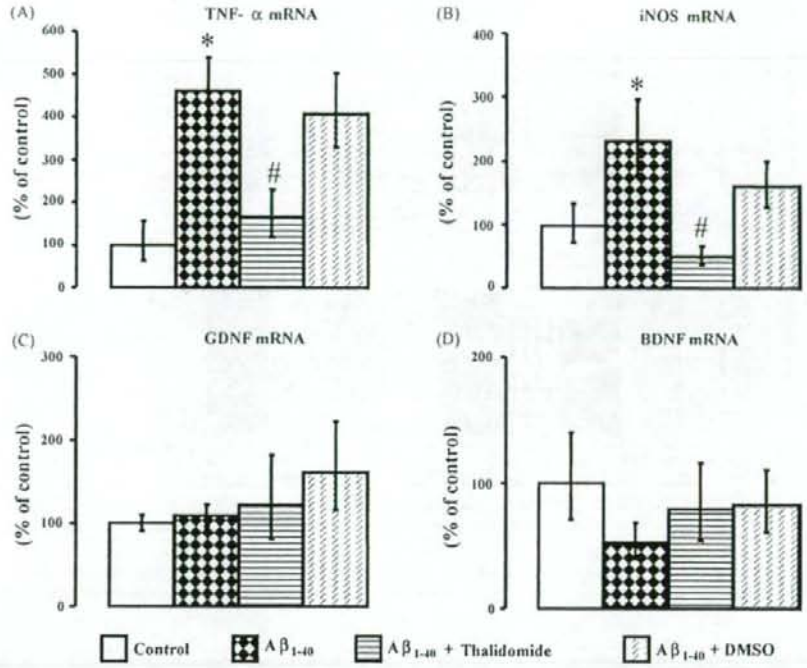

Fig. 3. Thalidomide suppressed the increase of TNF-α mRNA induced by $A\beta_{1-40}$. Thalidomide (20 mg/kg) was administrated *p.o.* one hour before the *i.c.v.*-injection of $A\beta_{1-40}$ in mice. A–D: Two hours after the injection of $A\beta_{1-40}$, the mRNA levels of TNF-α, iNOS, BDNF, and GDNF in the hippocampus were investigated by using real-time RT-PCR. Thalidomide suppressed the increase of TNF-α and iNOS mRNA induced by $A\beta_{1-40}$. The mRNA levels of BDNF and GDNF in the hippocampus were not changed either by $A\beta_{1-40}$ injection or thalidomide treatment. Data were presented as the mean ± S.E., $n = 4$, $^{*}p < 0.05$ vs. control, $^{\#}p < 0.05$ vs. $A\beta_{1-40}$; TNF-α: tumor necrosis factor-alpha; iNOS: inducible nitric oxide synthase; GDNF: glial cell-derived neurotrophic factor; BDNF: brain-derived neurotrophic factor; $A\beta_{1-40}$: Amyloid beta peptide (1–40). DMSO: dimethyl sulfoxide.

The selective inhibition of iNOS activity by aminoguanidine [14] or TNF-α (−/−) prevented $A\beta_{25-35}$ induced nitration of proteins in the hippocampus or the impairment of recognition memory in mice (Fig. 2C and D). The western blott analysis of protein nitration revealed only a single band for nitrated proteins at the size of 70 kDa. Through extensive studies with different anti-nitrotyrosine antibodies from different origin, we found that the detection of this single band is owing to the selectivity of the anti-nitrotyrosine mouse antibody [3]. These results, together with previous reports [2,13,36,65], confirmed that TNF-α is essential for the neurotoxicity of Aβ.

3.2. *Restraining TNF-α by thalidomide prevented Aβ-induced impairment of recognition memory*

The consistent involvement of TNF-α in the neurotoxicity of Aβ prompted us to examine an available candidate for anti-TNF-α remedy. Thalidomide, an immunomodulatory drug, has recently been suggested for the treatment of neurodegenerative disease as a selective inhibitor of TNF-α [21,60]. Thalidomide inhibits the synthesis of TNF-α through the degradation of mRNA [37]. We reexamined the selectivity of thalidomide-induced degradation of TNF-α mRNA. Thalidomide suppressed the increase of both TNF-α and iNOS mRNA induced by $A\beta_{1-40}$ (Fig. 3A and B). The decrease of iNOS mRNA might be due to the decrease of TNF-α [32]. The mRNA expressions of brain-derived neurotrophic factor (BDNF) and glial cell-derived neurotrophic factor (GDNF), however, were not affected either by $A\beta_{1-40}$ injection or thalidomide treatment (Fig. 3C and D). Either the daily treatment with thalidomide or the *i.c.v.*-injection of an anti-TNF-α antibody prevented the nitration of proteins in the hippocampus and the impairment of recognition memory induced by $A\beta_{25-35}$ or $A\beta_{1-40}$ (Fig. 4A and B). The preventive effects of the anti-TNF-α antibody was consistent with previous reports [36,65], and supported the validity of targeting TNF-α by thalidomide to prevent the neurotoxicity of Aβ.

4. Discussion

Providing effective medication or practical strategy for the treatment of the cognitive deficits in AD can have a dramatic effect on the quality of life of a patient.

As a strategy to prevent the cognitive decline in AD, anti-oxidants are well recommended based on the association of the increased cerebral oxidative damage with the progress of the disease [7,22,45]. The oxidative damage in the brain of AD is mostly ascribed to the increased level of Aβ that induces the peroxynitrite-mediated nitration of proteins and the resultant

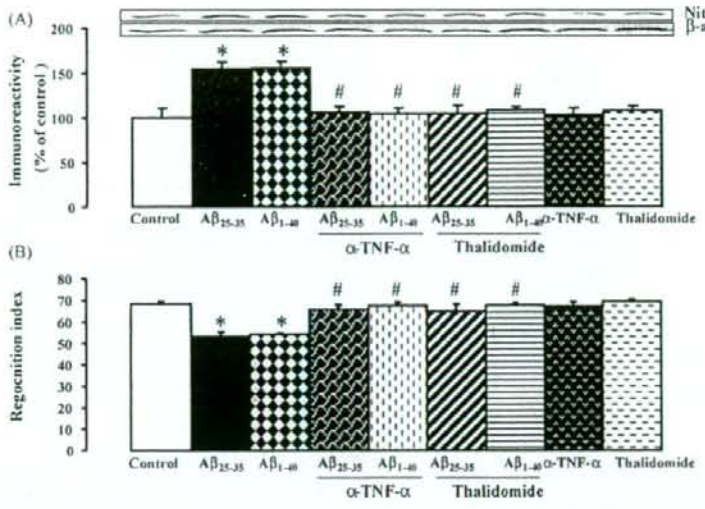

Fig. 4. Thalidomide prevented the nitration of proteins and the impairment of memory induced by Aβ. A–B: Thalidomide (20 mg/kg) was administrated *p.o.* daily until day 3 after the *i.c.v.*-injection of $A\beta_{25-35}$ or $A\beta_{1-40}$ (Day 0). An anti-TNF-α antibody (α-TNF-α) (10 ηg/mouse) was *i.c.v.*-injected 15 min prior to the injection of $A\beta_{25-35}$ or $A\beta_{1-40}$. Either the daily treatment with thalidomide or the *i.c.v.*-injection of α-TNF-α antibody prevented the nitration of proteins in the hippocampus (day 7) and the impairment of novel object recognition memory (day 8–10) induced by $A\beta_{25-35}$ or $A\beta_{1-40}$. Data were presented as the mean ± S.E., ($n = 4$ for E, $n = 10$ for F), $^{*}p < 0.05$ vs. control; $^{\#}p < 0.05$ vs. $A\beta_{25-35}$ or $A\beta_{1-40}$; α-TNF-α: anti-TNF-α antibody; $A\beta_{35-25}$: Amyloid beta peptide (35–25). $A\beta_{1-40}$: Amyloid beta peptide (1–40).

irreversible loss of function [9,10,46,53,54,67]. It is therefore thus suggested that preventing the formation of peroxynitrite should be the early strategy for interrupting the cognitive failure in AD. Peroxynitrite is the product of the inter-action of nitric oxide (NO) and superoxide [6,46]. Although the half-life of NO is extremely short, peroxynitrite could be formed at a rate more than three times faster than the scavenging of superoxide by superoxide dismutase, implying criticality of the over-produced NO [5]. The overproduction of NO by Aβ is ascribed to the overpexpression of iNOS [1,23,25,40,47,59,64]. The deletion of iNOS or inhibition of the activity prevents peroxynitrite-mediated damage or the impairment of memory induced by $A\beta_{1-40}$ [25,40,58]. Observation of iNOS overexpression in the brains of AD patients [33,61], supports an anti-iNOS strategy [40,59]. However, the involvement of iNOS in the important physiology of life such as sexuality and sleep in the recent reports makes the strategy less favorable [20,26]. Therefore, restraining the overproduction of iNOS without affecting its normal expression and function is desired. The involvement of the TNF-α in iNOS-mediated neurotoxicity of $A\beta_{1-40}$ [2,13,36,65], points out a better strategy of targeting TNF-α to prevent the iNOS-driven-peroxynitrite-mediated impairment of memory in the neurotoxicity of Aβ.

In the present study, we examined the feasibility of a strategy of targeting TNF-α for the prevention of Aβ-induced impairment of memory. To confirm the involvement of TNF-α in the Aβ-induced impairment of recognition memory, $A\beta_{25-35}$, the most toxic Aβ species detected in AD brain, and TNF-α (−/−) mouse were utilized. $A\beta_{25-35}$ did not induce the impairment of recognition memory in TNF-α (−/−) mouse. The serious involvement of TNF-α was consistent with the previous reports [2,13,36,65], and boosted the prospect of an anti-TNF-α strategy to prevent the neurotoxicity of Aβ. Considering the current availability for practice, thalidomide was selected due to its preferential degradative effect on the mRNA of TNF-α [32,37]. Thalidomide preferentially suppressed the increase of TNF-α mRNA and prevented the Aβ-induced impairment of recognition memory. An anti-TNF-α antibody also provided prevention against the impairment of recognition memory induced by Aβ, validating the usefulness of the strategy of targeting TNF-α.

A variety of inhibitory agents of the synthesis or the activity of TNF-α is widely investigated and currently used as remedy in practice [4,35]. However, the penetrating ability of the blood–brain-barrier (BBB) of these agents is one of the factors to challenge their application for the ailments in the central nervous system. With the ability of penetrating of BBB, thalidomide is recently emerged as good candidate for the treatment for neurodegenerative diseases due to its potent inhibitory property for the synthesis of TNF-α [21,24,60]. The drug has recently been reintroduced for treating leprosy, although once was withdrawn from the general market because of its catastrophic adverse effect of teratogenesis [31]. The treatment with thalidomide in AD may have very limited chance, in the elderly, of causing teratogenesis in the progeny. Since thalidomide has a neglectable weak inhibitory effect for NOS including iNOS [52], the attenuation of iNOS-related pathology could most likely be contributed by its inhibition of the synthesis of TNF-α [32]. These reports qualify thalidomide as an ideal agent for reducing the iNOS/peroxynitrite related pathology via restraining the increase of TNF-α without evidently harming the physiological function of iNOS. The neuroprotective effects of thalidomide

in an animal model of inflamed brain pathology of AD in a recent study also recommend and support the use of the drug [48].

In conclusion, the usefulness of restraining TNF-α by thalidomide to prevent Aβ-induced impairment of memory in mice would provide a practical fresh strategy for the management of cognitive deficits in AD.

Acknowledgements

This work was supported, in part, by the Japan–China Sasakawa Medical fellowship (for Tursun Alkam); by Uehara Memorial Foundation fellowship for Foreign Researchers in Japan (for Tursun Alkam); by a Grant-in-Aid for the 21st Century Center of Excellence Program "Integrated Molecular Medicine for Neuronal and Neoplastic Disorders" and "Academic Frontier Project for Private Universities (2007–2011) from the Ministry of Education, Culture, Sports, Science and Technology of Japan; by Comprehensive Research on Aging and Health from the Ministry of Health, Labor and Welfare of Japan; by Japan Canada Joint Health Research Program and Japan France Joint Health Research Program (Joint Project from Japan Society for the Promotion of Science); by International Research Project Supported by the Meijo Asian Research Center; and by a Smoking Research Foundation Grant for Biomedical Research and Takeda Science Foundation.

References

[1] Akama KT, Albanese C, Pestell RG, Van Eldik LJ. Amyloid beta-peptide stimulates nitric oxide production in astrocytes through an NFkappaB-dependent mechanism. Proc Natl Acad Sci USA 1998;95:5795–800.
[2] Akama KT, Van Eldik LJ. β-amyloid stimulation of inducible nitric-oxide synthase in astrocytes is interleukin-1beta- and tumor necrosis factor-alpha (TNF-α)-dependent, and involves a TNF-α receptor-associated factor- and NF kappa B-inducing kinase-dependent signaling mechanism. J Biol Chem 2000;275:7918–24.
[3] Alkam T, Nitta A, Mizoguchi H, Itoh A, Nabeshima T. A natural scavenger of peroxynitrites, rosmarinic acid, protects against impairment of memory induced by Abeta (25–35). Behav Brain Res 2007;180:139–45.
[4] Baugh JA, Bucala R. Mechanisms for modulating TNF alpha in immune and inflammatory disease. Curr Opin Drug Discov Devel 2001;4:635–50.
[5] Beckman JS. Peroxynitrite versus hydroxyl radical: the role of nitric oxide in superoxide-dependent cerebral injury. Ann NY Acad Sci 1994;738:69–75.
[6] Beckman JS, Crow JP. Pathological implications of nitric oxide, superoxide and peroxynitrite formation. Biochem Soc Trans 1993;21:330–4.
[7] Behl C, Moosmann B. Antioxidant neuroprotection in Alzheimer's disease as preventive and therapeutic approach. Free Radical Biol Med 2002;33:182–91.
[8] Bruunsgaard H, Andersen-Ranberg K, Jeune B, Pedersen AN, Skinhoj P, Pedersen BK. A high plasma concentration of TNF-α is associated with dementia in centenarians. J Gerontol A Biol Sci Med Sci 1999;54:357–64.
[9] Butterfield DA, Drake J, Pocernich C, Castegna A. Evidence of oxidative damage in Alzheimer's disease brain: central role for amyloid beta-peptide. Trends Mol Med 2001;7:548–54.
[10] Castegna A, Thongboonkerd V, Klein JB, Lynn B, Markesbery WR, Butterfield DA. Proteomic identification of nitrated proteins in Alzheimer's disease brain. J Neurochem 2003;85:1394–401.
[11] Chan ED, Riches DW. Potential role of the JNK/SAPK signal transduction pathway in the induction of iNOS by TNF-alpha. Biochem Biophys Res Commun 1998;253:790–6.
[12] Chung F, Lu J, Palmer BD, Kestell P, Browett P, Baguley BC, et al. Thalidomide pharmacokinetics and metabolite formation in mice, rabbits, and multiple myeloma patients. Clin Cancer Res 2004;10:5949–56.
[13] Combs CK, Karlo JC, Kao SC, Landreth GE. β-Amyloid stimulation of microglia and monocytes results in TNF-α dependent expression of inducible nitric oxide synthase and neuronal apoptosis. J Neurosci 2001;21:1179–88.
[14] Corbett JA, McDaniel ML. Selective inhibition of inducible nitric oxide synthase by aminoguanidine. Method Enzymol 1996;268:398–408.
[15] Dodart JC, Bales KR, Gannon KS, Greene SJ, DeMattos RB, Mathis C, et al. Immunization reverses memory deficits without reducing brain Abeta burden in Alzheimer's disease model. Nat Neurosci 2002;5:452–7.
[16] Ennaceur A, Delacour J. A new one-trial test for neurobiological studies of memory in rats. 1: Behavioral data. Behav Brain Res 1998;31:47–59.
[17] Fillit H, Ding WH, Buee L, Kalman J, Altstiel L, Lawlor B, et al. Elevated circulating tumor necrosis factor levels in Alzheimer's disease. Neurosci Lett 1991;129:318–20.
[18] Glenner GG, Wong CW. Alzheimer's disease: initial report of the purification and characterization of a novel cerebrovascular amyloid protein. Biochem Biophys Res Commun 1984;120:885–90.
[19] Golde TE. Alzheimer disease therapy: can the Amyloid cascade be halted? J Clin Invest 2003;111:11–8.
[20] Gonzalez-Cadavid NF, Rajfer J. The pleiotropic effects of inducible nitric oxide synthase (iNOS) on the physiology and pathology of penile erection. Curr Pharm Des 2005;11:4041–6.
[21] Greig NH, Giordano T, Zhu X, Yu QS, Perry TA, Holloway HW, et al. Thalidomide-based TNF-alpha inhibitors for neurodegenerative diseases. Acta Neurobiol Exp 2004;64:1–9.
[22] Grundman M, Grundman M, Delaney P. Antioxidant strategies for Alzheimer's disease. Proc Nutr Soc 2002;61:191–202.
[23] Hu J, Akama KT, Krafft GA, Chromy BA, Van Eldik LJ. Amyloid-beta peptide activates cultured astrocytes: morphological alterations, cytokine induction and nitric oxide release. Brain Res 1998;785:195–206.
[24] Huang YJ, Liao JF, Tsai TH. Concurrent determination of thalidomide in rat blood, brain and bile using multiple microdialysis coupled to liquid chromatography. Biomed Chromatogr 2005;19:488–93.
[25] Ishii K, Muelhauser F, Liebl U, Picard M, Kühl S, Penke B, et al. Subacute NO generation induced by Alzheimer's beta-amyloid in the living brain: reversal by inhibition of the inducible NO synthase. FASEB J 2000;14:1485–9.
[26] Kalinchuk AV, Stenberg D, Rosenberg PA, Porkka-Heiskanen T. Inducible and neuronal nitric oxide synthases (NOS) have complementary roles in recovery sleep induction. Eur J Neurosci 2006;24:1443–56.
[27] Keller JN. Oxidative damage and oxidative stress in Alzheimer's disease. Res Pract Alzheimer's Dis 2006;11:110–4.
[28] Koppal T, Drake J, Yatin S, Jordan B, Varadarajan S, Bettenhausen L, et al. Peroxynitrite-induced alterations in synaptosomal membrane proteins: insight into oxidative stress in Alzheimer's disease. J Neurochem 1999;72:310–7.
[29] Kubo T, Nishimura S, Kumagae Y, Kaneko I. In vivo conversion of racemized beta-amyloid ([D-Ser 26]A beta 1–40) to truncated and toxic fragments ([D-Ser 26]A beta 25–35/40) and fragment presence in the brains of Alzheimer's patients. J Neurosci Res 2002;70:474–83.
[30] Lahiri DK, Farlow MR, Sambamurti K, Greig NH, Giacobini E, Schneider LS. A critical analysis of new molecular targets and strategies for drug developments in Alzheimer's disease. Curr Drug Target 2003;4:97–112.
[31] Lash JW, Saxén L. Human Teratogenesis: invitro studies on thalidomide-inhibited chondrogenesis. Dev Biol 1972;28:61–70.
[32] Lopez-Talavera JC, Cadelina G, Olchowski J, Merrill W, Groszmann RJ. Thalidomide inhibits tumor necrosis factor alpha, decreases nitric oxide synthesis, and ameliorates the hyperdynamic circulatory syndrome in portal-hypertensive rats. Hepatology 1996;23:1616–21.
[33] Luth HJ, Munch G, Arendt T. Aberrant expression of NOS isoforms in Alzheimer's disease is structurally related to nitrotyrosine formation. Brain Res 2002;953:135–43.
[34] Maurice T, Lockart BP, Private A. Amnesia induced by centrally administered β-amyloid peptides involves cholinergic dysfunction. Brain Res 1996;706:181–93.

[35] McDermott MF. TNF and TNFR biology in health and disease. Cell Mol Biol 2001;47:619–35.
[36] Medeiros R, Prediger RD, Passos GF, Pandolfo P, Duarte FS, Franco JL, et al. Connecting TNF-alpha signaling pathways to iNOS expression in a mouse model of Alzheimer's disease: relevance for the behavioral and synaptic deficits induced by amyloid beta protein. J Neurosci 2007;27:5394–404.
[37] Moreira AL, Sampaio EP, Zmuidzinas A, Frindt P, Smith KA, Kaplan G. Thalidomide exerts its inhibitory action on tumor necrosis factor alpha by enhancing mRNA degradation. J Exp Med 1993;177:1675–80.
[38] Mouri A, Noda Y, Hara H, Mizoguchi H, Tabira T, Nabeshima T. Oral vaccination with a viral vector containing Abeta cDNA attenuates age-related Abeta accumulation and memory deficits without causing inflammation in a mouse Alzheimer model. FASEB J 2007;21:2135–48.
[39] Nabeshima T, Nitta A. Memory impairment and neuronal dysfunction induced by β-amyloid protein in rats. Tohoku J Exp Med 1994;174:241–9.
[40] Nathan C, Calingasan N, Nezezon J, Ding A, Lucia MS, La Perle K, et al. Protection from Alzheimer's-like disease in the mouse by genetic ablation of inducible nitric oxide synthase. J Exp Med 2005;202:1163–9.
[41] Nitta A, Itoh A, Hasegawa T, Nabeshima T. β-Amyloid protein-induced Alzheimer's disease animal model. Neurosci Lett 1994;170:63–6.
[42] Olney JW, Wozniak DF, Farber NB. Excitotoxic neurodegeneration in Alzheimer disease. New hypothesis and new therapeutic strategies. Arch Neurol 1997;54:1234–40.
[43] Perry RT, Collins JS, Wiener H, Acton R, Go RC. The role of TNF and its receptors in Alzheimer's disease. Neurobiol Aging 2001;22:873–83.
[44] Pike CJ, Walencewicz-Wasserman AJ, Kosmoski J, Cribbs DH, Glabe CG, Cotman CW. Structure-activity analyses of Abeta peptides: contributions of the β25–35 region to aggregation and neurotoxicity. J Neurochem 1995;64:253–65.
[45] Praticò D, Clark CM, Liun F, Rokach J, Lee VY, Trojanowski JQ. Increase of brain oxidative stress in mild cognitive impairment: A possible predictor of Alzheimer's disease. Arch Neurol 2002;59:972–6.
[46] Reiter CD, Teng RJ, Beckman JS. Superoxide reacts with nitric oxide to nitrate tyrosine at physiological pH via peroxynitrite. J Biol Chem 2000;275:32460–6.
[47] Rodrigo J, Fernández-Vizarra P, Castro-Blanco S, Bentura ML, Nieto M, Gómez-Isla T, et al. Nitric oxide in the cerebral cortex of amyloid-precursor protein (SW) Tg2576 transgenic mice. Neuroscience 2004;128:73–89.
[48] Ryu JK, McLarnon JG. Thalidomide inhibition of perturbed vasculature and glial-derived tumor necrosis factor-alpha in an animal model of inflamed Alzheimer's disease brain. Neurobiol Dis 2007 [Epub ahead of print].
[49] Selkoe DJ. The molecular pathology of Alzheimer's disease. Neuron 1991;6:487–98.
[50] Selkoe DJ. Deciphering the genesis and fate of amyloid beta-protein yields novel therapies for Alzheimer disease. J Clin Invest 2002;110:1375–81.
[51] Shalit F, Sredni B, Rosenblatt-Bin H, Kazimirsky G, Brodie C, Huberman M. Beta-amyloid peptide induces tumor necrosis factor-alpha and nitric oxide production in murine macrophage cultures. Neuroreport 1997;8:3577–80.
[52] Shimazawa R, Sano H, Tanatani A, Miyachi H, Hashimoto Y. Thalidomide as a nitric oxide synthase inhibitor and its structural development. Chem Pharm Bull 2004;52:498–9.
[53] Smith MA, Perry G, Richey PL, Sayre LM, Anderson VE, Beal MF, et al. Oxidative damage in Alzheimer's. Nature 1996;382:120–1.
[54] Smith MA, Richey Harris PL, Sayre LM, Beckman JS, Perry G. Widespread peroxynitrite-mediated damage in Alzheimer's disease. J Neurosci 1997;17:2653–7.
[55] Taniguchi T, Tanaka M, Ikeda A, Momotani E, Sekikawa K. Failure of germinal center formation and impairment of response to endotoxin in tumor necrosis factor-alpha deficient mice. Lab Invest 1997;77:647–58.
[56] Tarkowski E, Andreasen N, Tarkowski A, Blennow K. Intrathecal inflammation precedes development of Alzheimer's disease. J Neurol Neurosurg Psychiat 2003;74:1200–5.
[57] Tohgi H, Abe T, Yamazaki K, Murata T, Ishizaki E, Isobe C. Alterations of 3 nitrotyrosine concentration in the cerebrospinal fluid during aging and in patients with Alzheimer's disease. Neurosci Lett 1999;269:52–4.
[58] Tran MH, Yamada K, Nakajima A, Mizuno M, He J, Kamei H, et al. Tyrosine nitration of a synaptic protein synaptophysin contributes to amyloid β-peptide-induced cholinergic dysfunction. Mol Psychiat 2003;8:407–12.
[59] Tran MH, Yamada K, Olariu A, Mizuno M, Ren XH, Nabeshima T. Amyloid beta-peptide induces nitric oxide production in rat hippocampus: association with cholinergic dysfunction and amelioration by inducible nitric oxide synthase inhibitors. FASEB J 2001;15:1407–9.
[60] Tweedie D, Sambamurti K, Greig NH. TNF-alpha inhibition as a treatment strategy for neurodegenerative disorders: new drug candidates and targets. Curr Alzheimer Res 2007;4:378–85.
[61] Vodovotz Y, Lucia MS, Flanders KC, Chesler L, Xie QW, Smith TW, et al. Inducible nitric oxide synthase in tangle-bearing neurons of patients with Alzheimer's disease. J Exp Med 1996;184:1425–33.
[62] Wada R, Tifft CJ, Proia RL. Microglial activation precedes acute neurodegeneration in Sandhoff disease and is suppressed by bone marrow transplantation. Proc Natl Acad Sci USA 2000;97:10954–9.
[63] Walsh DM, Selkoe DJ. Deciphering the molecular basis of memory failure in Alzheimer's disease. Neuron 2004;44:181–93.
[64] Wang Q, Rowan MJ, Anwyl R. β-Amyloid-mediated inhibition of NMDA receptor-dependent long-term potentiation induction involves activation of microglia and stimulation of inducible nitric oxide synthase and superoxide. J Neurosci 2004;24:6049–56.
[65] Wang Q, Wu J, Rowan MJ, Anwyl R. α-amyloid inhibition of long-term potentiation is mediated via tumor necrosis factor. Eur J Neurosci 2005;22:2827–32.
[66] Wyss-Coray T. Inflammation in Alzheimer disease: driving force, bystander or beneficial response? Nat Med 2006;12:1005–15.
[67] Xie Z, Wei M, Morgan TE, Fabrizio P, Han D, Finch CE, et al. Peroxynitrite mediates neurotoxicity of amyloid beta-peptide1-42 and lipopolysaccharide-activated microglia. J Neurosci 2002;22:3484–92.
[68] Zameer A, Schulz P, Wang MS, Sierks MR. Single chain Fv antibodies against the 25-35 Aβ fragments inhibit aggregation and toxicity of Aβ42. Biochemistry 2006;45:11532–9.
[69] Zeng C, Lee JT, Chen H, Chen S, Hsu CY, Xu J. Amyloid-β peptide enhances tumor necrosis factor-alpha-induced iNOS through neutral sphingomyelinase/ceramide pathway in oligodendrocytes. J Neurochem 2005;94:703–12.

Cell Transplantation, Vol. 17, pp. 223–229, 2008

0963-6897/08 $90.00 + .00
E-ISSN 1555-3892
www.cognizantcommunication.com

Bcl-2 Protects Tubular Epithelial Cells From Ischemia Reperfusion Injury by Inhibiting Apoptosis

Chigure Suzuki,* Yoshitaka Isaka,*† Shigeomi Shimizu,‡ Yoshihide Tsujimoto,‡ Yoshitsugu Takabatake,* Takahito Ito,* Shiro Takahara,† and Enyu Imai*

*Department of Nephrology, Osaka University Graduate School of Medicine, Suita, Osaka, Japan
†Department of Advanced Technology for Transplantation, Osaka University Graduate School of Medicine, Suita, Osaka, Japan
‡Department of Post-Genomics & Diseases, Osaka University Graduate School of Medicine, Suita, Osaka, Japan

Ischemia followed by reperfusion leads to severe organ injury and dysfunction. Inflammation is considered to be the most important cause of graft dysfunction in kidney transplantation subjected to ischemia. The mechanism that triggers inflammation and renal injury after ischemia remains to be elucidated; however, cellular stress may induce apoptosis during the first hours and days after transplantation, which might play a crucial role in early graft dysfunction. Bcl-2 is known to inhibit apoptosis induced by the etiological factors promoting ischemia and reperfusion injury. Accordingly, we hypothesized that an augmentation of the anti-apoptotic factor Bcl-2 may thus protect tubular epithelial cells by inhibiting apoptosis, thereby ameliorating the subsequent tubulointerstitial injury. We examined the effects of Bcl-2 overexpression on ischemia-reperfusion (I/R) injury using Bcl-2 transgenic mice (Bcl-2 TG) and their wild-type littermates (WT). To investigate the effects of I/R injury, the left renal artery and vein were clamped for 45 min, followed by reperfusion for 0–96 h. Bcl-2 TG exhibited decreased active caspase protein in the tubular cells, which led to a reduction in TUNEL-positive apoptotic cells. Consequently, interstitial fibrosis and phenotypic changes were ameliorated in Bcl-2 TG. In conclusion, Bcl-2 augmentation protected renal tubular epithelial cells from I/R, and subsequent interstitial injury by inhibiting tubular apoptosis.

Key words: Bcl-2; Apoptosis; TGF-β; Ischemia-reperfusion injury

INTRODUCTION

Both clinical and experimental evidence suggests that ischemia-reperfusion (I/R) injury to kidney grafts may influence both early and late transplant function (23). Ischemia followed by reperfusion is closely related to the pathogenesis of early graft damage. Overall, ischemia in a kidney graft is the sum of possible transient warm ischemia during allograft removal from the donor and cold ischemia associated with preservation and storage (19). Reperfusion, which is critical to the viability of the organ, may also induce additional damage (15). Prolonged exposure of the donor kidney to warm and/or cold ischemia increases the incidence of delayed graft function upon transplantation and primes a programmed process within the kidney, which may lead to chronic and progressive lesions (18). Several studies have reported the initial I/R injury to possibly significantly affect the graft outcome, thus suggesting that the long-term graft function might improve by manipulating the early graft injury induced by I/R (8).

I/R injury at the renal level is characterized by apoptosis of tubular cells and interstitial inflammation. Renal ischemia induces tubular cell injury with decreasing levels of ATP, increasing levels of calcium, and an alteration in the membrane lipid and enzyme activity (7). Reperfusion of the ischemic organ exacerbates ischemic injury by producing cytotoxic oxygen species and free radicals (9). In addition, a deleterious role for the inflammatory response in I/R-induced organ damage has also been suggested by the enhanced expression of adhesion molecules and proinflammatory mediators (cytokines, chemokines), the activation of the complement system, the priming of the coagulation cascade, and the subsequent leukocyte infiltration (5,25).

Apoptosis is a precisely regulated process and the molecular regulation of cell death has recently been reported to originate with the *bcl-2* gene family. Bcl-2 is known to inhibit the apoptosis induced by etiological factors promoting ischemia and reperfusion injury (14). Bcl-2 allows clonal survival after cell stress is removed (14). More importantly, human *bcl-2*-gene transfection

Received February 5, 2007; accepted September 30, 2007.
Address correspondence to Yoshitaka Isaka, Department of Advanced Technology for Transplantation, Osaka University Graduate School of Medicine, Suita, Osaka 565-0871, Japan. Tel: +81-6-6879-3746; Fax: +81-6-6879-3749; E-mail: isaka@att.med.osaka-u.ac.jp

resulted in the prevention of hypoxic cell death in liver (24). Therefore, Bcl-2 is a good candidate to inhibit programmed cell death in the context of I/R injury. Organ treatment modalities, which may reduce the consequences of I/R injuries, are thus considered to play a critical role in increasing graft survival, particularly with the present shortage of donor organs.

Therefore, we investigated the effects of Bcl-2 overexpression on tubular apoptosis and subsequent tubulointerstitial damage after I/R injury, using *bcl-2* transgenic mice.

MATERIALS AND METHODS

Experimental Design

In order to confirm the protective effects of Bcl-2 on tubular epithelial cells, we employed Bcl-2 transgenic mice (Bcl-2 TG) harboring the human *bcl-2* gene (12). In this transgenic mouse, human *bcl-2* was driven by the regulatory sequences of the rat *L-type pyruvate kinase* gene, which encodes a glycolytic enzyme expressed mainly in hepatocytes, enterocytes, and proximal tubular cells. Three- to 4-month-old Bcl-2 TG or WT mice were maintained under standard conditions until the experiments were performed. All studies were performed in accordance with the principles of the Guidelines on Animal Experimentation of Osaka University. All mice were anesthetized with an IP injection of sodium pentobarbital (30 mg/kg). To investigate the effects of I/R injury, Bcl-2 TG or WT were allowed to stabilize for 30 min before being subjected to 45 min of bilateral renal occlusion using artery clips to clamp the renal pedicles. Occlusion was visually confirmed by a paling in the kidney color. Reperfusion was initiated by removing the artery clips and it was visually confirmed when blushing was noted. The mice were sacrificed at 3, 24, 48, and 96 h after reperfusion. The sham-operated mice were also sacrificed as normal controls. Left kidneys were harvested after perfusing with phosphate-buffered saline (PBS).

Antibodies

To identify myofibroblasts, we used anti-human α-smooth muscle actin (α-SMA) antibody (EPOS System: Dako, Hamburg, Germany). The localization of active caspase-3 protein expression was determined by immunohistochemistry using antiactive caspase antibody (1:250 dilution; Promega, Madison, WI). To evaluate the caspase activity by a Western blot analysis, we used caspase-3 antibody (1:1000 dilution; BD Biosciences San Jose, CA). To examine the mechanisms of interstitial fibrosis, a potent fibrogenic growth factor was examined using anti-TGF-β1 antibody (1:50 dilution; Santa Cruz Biotechnology, Santa Cruz, CA).

Morphology and Immunohistochemical Staining

Tissue samples were fixed in 4% (w/v) buffered paraformaldehyde (PFA) for 16 h and then were embedded in paraffin. Tissue sections (4 μm) were mounted on silane (2% 3-aminopropyltriethoxysilane)-coated slides (Muto Pure Chemicals, Tokyo, Japan), deparaffinized with xylene, and stained with periodic acid-Schiff (PAS) and Masson's Trichrome. Immunohistochemical staining was performed using the Envision system (Dako), according to the manufacturer's instructions. Endogenous peroxidase activity was blocked with 3% H_2O_2 for 5 min. The first antibodies were diluted in 1.5% goat serum albumin in PBS at specific concentrations as described above, and incubated for 24 h at 4°C. This was followed by incubation with suitable secondary antibodies. Antigen retrieval was performed for 2 min in preheated 10 mmol/L sodium citrate (pH 7) using a microwave oven.

Terminal Deoxynucleotidyltransferase-Mediated dUTP Nick End-Labeling (TUNEL) Staining

TUNEL staining was performed using the in situ Apoptosis Detection Kit (Takara Bio, Otsu, Japan), according to the manufacturer's instructions. Briefly, the sections were deparaffinized and subjected to antigen retrieval in preheated 10 mmol/L sodium citrate (pH 7) using a steamer for 40 min. They were then incubated with 3% H_2O_2 for 10 min, which was followed by incubation with TdT enzyme solution for 90 min at 37°C. The reaction was terminated by incubation in a stop/wash buffer for 30 min at 37°C.

Western Blot Analysis

The tissue specimen was homogenized in RIPA buffer (10 mM Tris, pH 7.4, 150 mM NaCl, 1% NP-40,1 mM EDTA) containing 1% SDS and sonicated. The lysate was centrifuged at 15,000 rpm for 10 min at 4°C and the supernatant was collected. The protein concentration in each renal tissue lysate was determined using a BCA protein assay kit (Pierce Biotechnology, Rockford, IL). The lysate was mixed with 0.5 volume of 5× SDS sample buffer and boiled for 15 min. Next, 20 μg of protein was loaded onto each lane and electrophoresed on a 15% SDS polyacrylamide gel, followed by blotting on a PVDF transfer membrane (Amersham Biosciences, UK). The filter was blocked with 5% (w/v) nonfat milk or 1% BSA in 10 mM Tris-buffered saline with 0.1% Tween-20 (TBS-T), followed by overnight incubation at 4°C with diluted primary antibodies in TBS-T or blocking buffer. After washing three times in TBS-T, the filter was incubated with secondary antibody (1:1000) (Cell Signaling) in TBS-T for 30 min at room temperature and developed to detect specific pro-

tein bands using ECL reagents (Amersham Bioscience Corp., Piscataway, NJ).

RESULTS

Effects on Histological Changes

To investigate the role of apoptosis on I/R-induced kidney injury, WT mice and Bcl-2 transgenic mice, in which human Bcl-2 is highly expressed in tubular epithelial cells (Fig. 1), were treated with I/R, and the morphological changes were assessed. PAS staining of the kidney sections obtained from WT at 48 h (Fig. 2a after I/R injury revealed marked disruption of normal tubular morphology, including the widespread degeneration of tubular architecture, tubular dilatation, swelling, and luminal congestion with loss of the brush border. Furthermore, interstitial fibrosis was observed at 96 h after I/R injury in WT (Fig. 2b). In contrast, Bcl-2 TG exhibited reduced severity with regard to the characteristic histological changes of I/R injury, including tubular atrophy (Fig. 2c). Importantly, Bcl-2 TG showed minimal interstitial fibrosis at 96 h after I/R injury (Fig. 2d), thus indicating that Bcl-2 dramatically inhibited I/R-induced kidney damage.

Effects on Interstitial Phenotypic Changes in Kidney After I/R Injury

In order to detect interstitial myofibroblasts, which are associated with interstitial damage and fibrosis, the expression of α-SMA was examined immunohistochemically. As shown in Figure 3, the interstitial expression of α-SMA increased at 96 h after I/R injury in WT, while it was significantly suppressed and limited to the blood vessels in Bcl-2 TG (Fig. 3b), which was consistent with the results obtained from PAS staining (Fig. 2).

Effects on Tubular Apoptosis in the I/R Injury Kidney

The inhibition of I/R-induced kidney injury by Bcl-2 overexpression proposed the possibility that apoptosis plays a crucial role in I/R injury. In fact, the number of TUNEL-positive, apoptotic cells increased among the tubular epithelial cells at 96 h after I/R injury in WT (Fig. 4a), and decreased in Bcl-2 TG (Fig. 4b). Consistently, the distribution of active caspase-3 was scattered in the tubular epithelial cells and in the interstitial area (Fig. 5a) in WT, and positively stained cells often showed the morphological changes of apoptosis (i.e., shrunken cells with condensed nuclei). In contrast, the active caspase-3-positive cells were little observed in Bcl-2 TG (Fig. 5b). Similar results were also observed when caspase-3 activation was assessed by a Western blot analysis (Fig. 5c). These data indicated that I/R of kidney induced apoptosis in tubular epithelial cells, which was markedly prevented by Bcl-2.

Effects on Interstitial Fibrosis in Kidney After I/R Injury

Finally, to evaluate the I/R-induced kidney injury, and to examine the correlation between apoptosis and kidney injury, the extent of interstitial fibrotic change in I/R kidneys was investigated by performing histological analysis using Masson's trichrome staining. The size of the fibrotic lesions in the interstitium was determined in stained sections. Kidney sections from WT at 96 h after I/R injury showed an expanded interstitium when compared with normal kidney (data not shown). In contrast, the interstitial fibrotic area was significantly suppressed in I/R kidneys from Bcl-2 TG.

As a smaller fibrotic area was observed in Bcl-2 TG, we examined the expression of TGF-β, a potent fibrotic growth factor, in I/R kidneys. Immunohistochemical

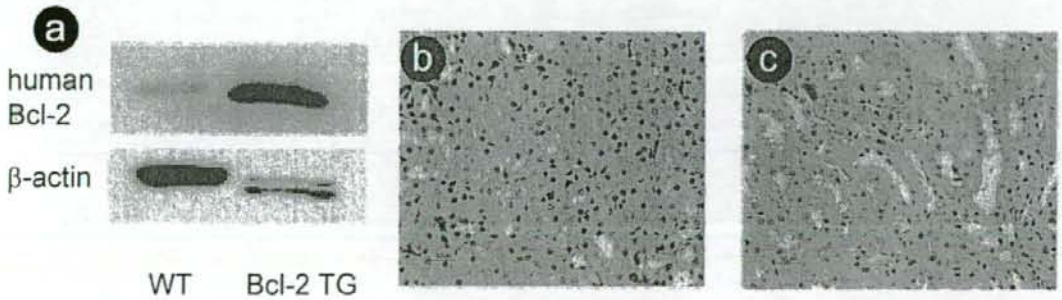

Figure 1. A Western blot analysis demonstrated that human Bcl-2 is highly expressed in Bcl-2 transgenic mice (a). Immunohistological staining showed that human Bcl-2 is not expressed in WT mice (b). Human Bcl-2 is expressed in tubular epithelial cells in Bcl-2 TG (c).

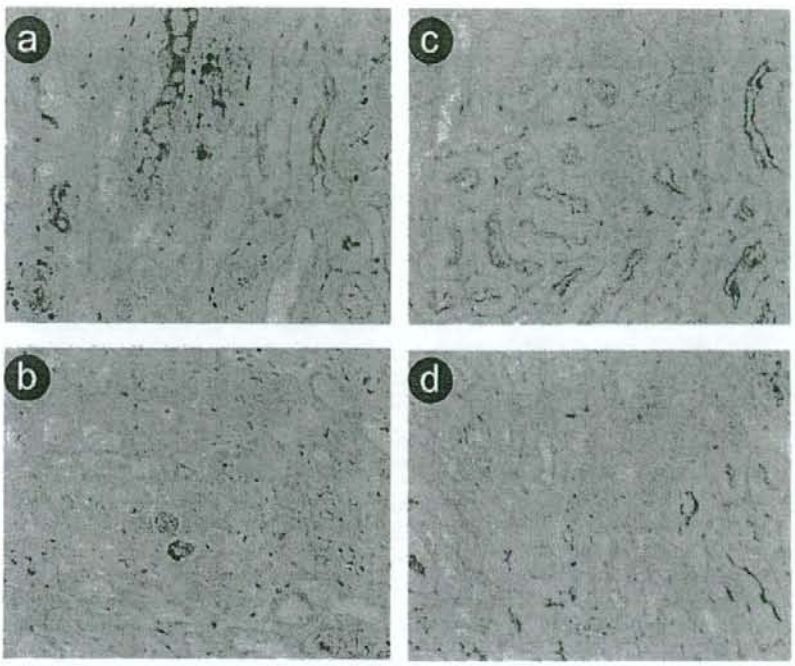

Figure 2. Representative morphological changes after PAS staining are shown in WT (a, b) and Bcl-2 TG (c, d) at 48 h (a, c) and 96 h (b, d) following I/R injury (original magnification 400×).

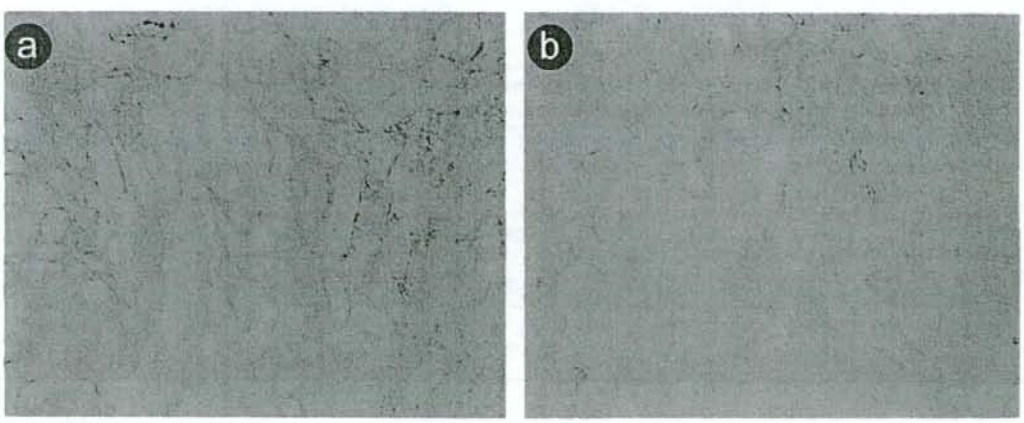

Figure 3. Effects of Bcl-2 on phenotypic alteration after I/R injury. α-SMA was strongly expressed in the interstitial area after I/R injury in WT (a), but was limited to blood vessels in Bcl-2 TG (b) (original magnification 400×).

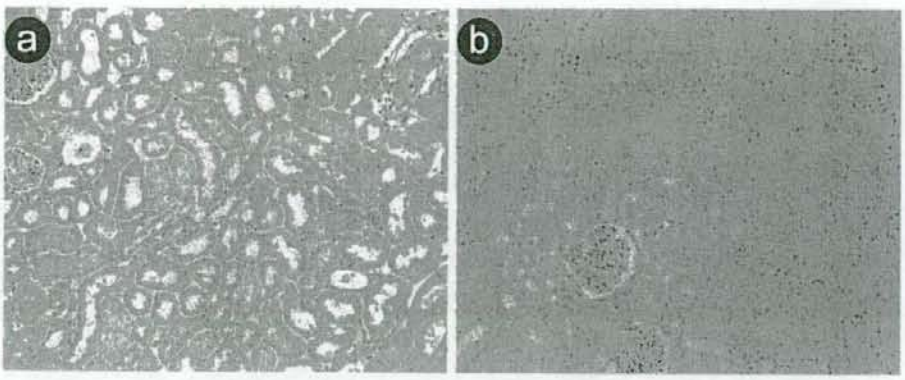

Figure 4. Effects of Bcl-2 on apoptosis at 96 h after I/R injury. Dark brown dots correspond to representative TUNEL-positive nuclei. (a) WT, (b) Bcl-2 TG (original magnification 400×).

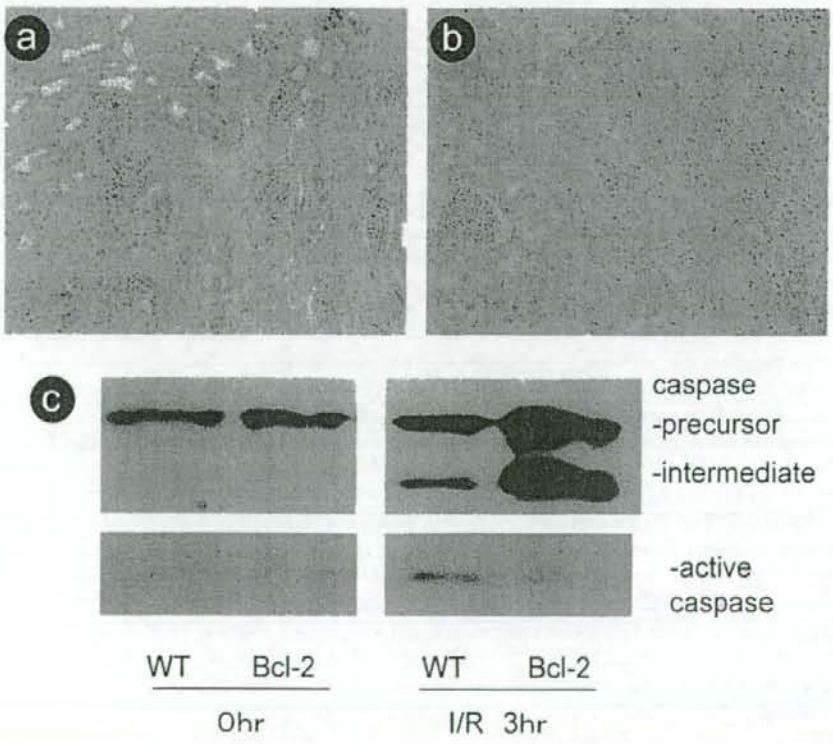

Figure 5. Effects of Bcl-2 on active caspase-3 expression at 3 h after I/R injury. Active caspase-3 was expressed in tubular epithelial cells at 3 h after I/R injury in WT (a), but not in Bcl-2 TG (b) (original magnification 400×). A Western blot analysis demonstrated that the active form of caspase-3 was diminished in Bcl-2 TG compared to WT.

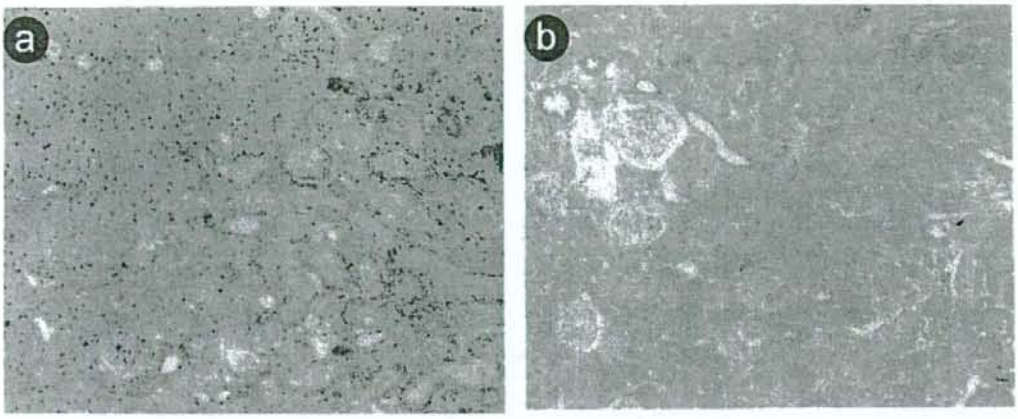

Figure 6. Effects of Bcl-2 on TGF-β expression. TGF-β was expressed in tubular epithelial cells after I/R injury in WT (a), but not in Bcl-2 TG (b) (original magnification 400×).

staining confirmed that the expression of TGF-β was upregulated in the tubular epithelial cells in I/R kidney from WT (Fig. 6a), and that this expression was weak in I/R kidney from Bcl-2 TG (Fig. 6b).

DISCUSSION

We examined whether Bcl-2 overexpression has a therapeutic effect on tubulointerstitial injury in a mouse model of I/R injury. We hypothesized that apoptosis following I/R constitutes a potential trigger of inflammation, and we studied this possibility by using Bcl-2 TG in a model of renal I/R. Evidence for the early involvement of apoptosis is provided by the characteristic morphological features in tubular epithelial cells, and the increase in TUNEL-positive cells, as well as increased active caspase-3 expression, in kidneys after I/R injury. These findings are in line with various in vivo and in vitro reports showing that renal apoptosis after ischemia is induced by hypoxia (1) and ATP depletion (13). Furthermore, during I/R-induced inflammation at day 1, upregulated Fas (16) and TNF-α (3) are associated with I/R-induced apoptosis. However, Bcl-2 TG exhibited decreased active caspase protein in tubular cells, and thus a reduction in the number of TUNEL-positive apoptotic cells. Consequently, both interstitial fibrosis and phenotypic changes were ameliorated in Bcl-2 TG.

Apoptosis represents a highly controlled process that is regulated by various factors (21). It is reported that Bcl-2 blocks cell death and modulates intracellular signaling events. In this regard, it has been shown that Bcl-2 inhibits depletion of Ca^{2+} from the endoplasmic reticulum (4) as well as the generation of reactive oxygen species and free radicals (10). Furthermore, it significantly impedes the downstream oxidative damage resulting from the radicals after they have been generated (11). An increase of mitochondrial membrane permeability is one of the key events in apoptotic death (20,22). The mitochondrial membrane permeability transition (MPT) is a Ca^{2+}-dependent increase of mitochondrial membrane permeability that leads to loss of $\Delta\psi$, mitochondrial swelling, and rupture of the outer mitochondrial membrane (26). The antiapoptotic Bcl-2 has the ability to block the MPT, and can therefore block MPT-dependent necrosis in addition to their well-established ability to inhibit apoptosis (20,22). As a result, the ability of Bcl-2 to protect against the damaging effects involved in ischemia and reperfusion injury makes Bcl-2 an appropriate candidate to inhibit apoptosis in renal transplantation.

We observed the upregulation of TGF-β in tubular epithelial cells in WT after I/R, as reported previously (6), while TGF-β expression was suppressed in Bcl-2 TG. Maintained upregulation of TGF-β expression is injurious, and is associated with the activation of fibroblasts and macrophages in the renal interstitium, and with the deposition of collagen and renal fibrosis (2). In addition, we observed α-SMA expression and fibrosis in the interstitium of WT after I/R injury, while α-SMA expression and fibrosis in the interstitium was suppressed in Bcl-2 TG. In our model, the precise relationship between Bcl-2 and tubulointerstitial injury remains unclear; however, one possible mechanism is that the Bcl-2-mediated protection from apoptosis results in the reduction of the TGF-β expression in tubular epithelial cells, which induces epithelial-mesenchymal transition (EMT) and subsequent α-SMA expression and interstitial fibrosis (17).

In line with previous findings, the results of this